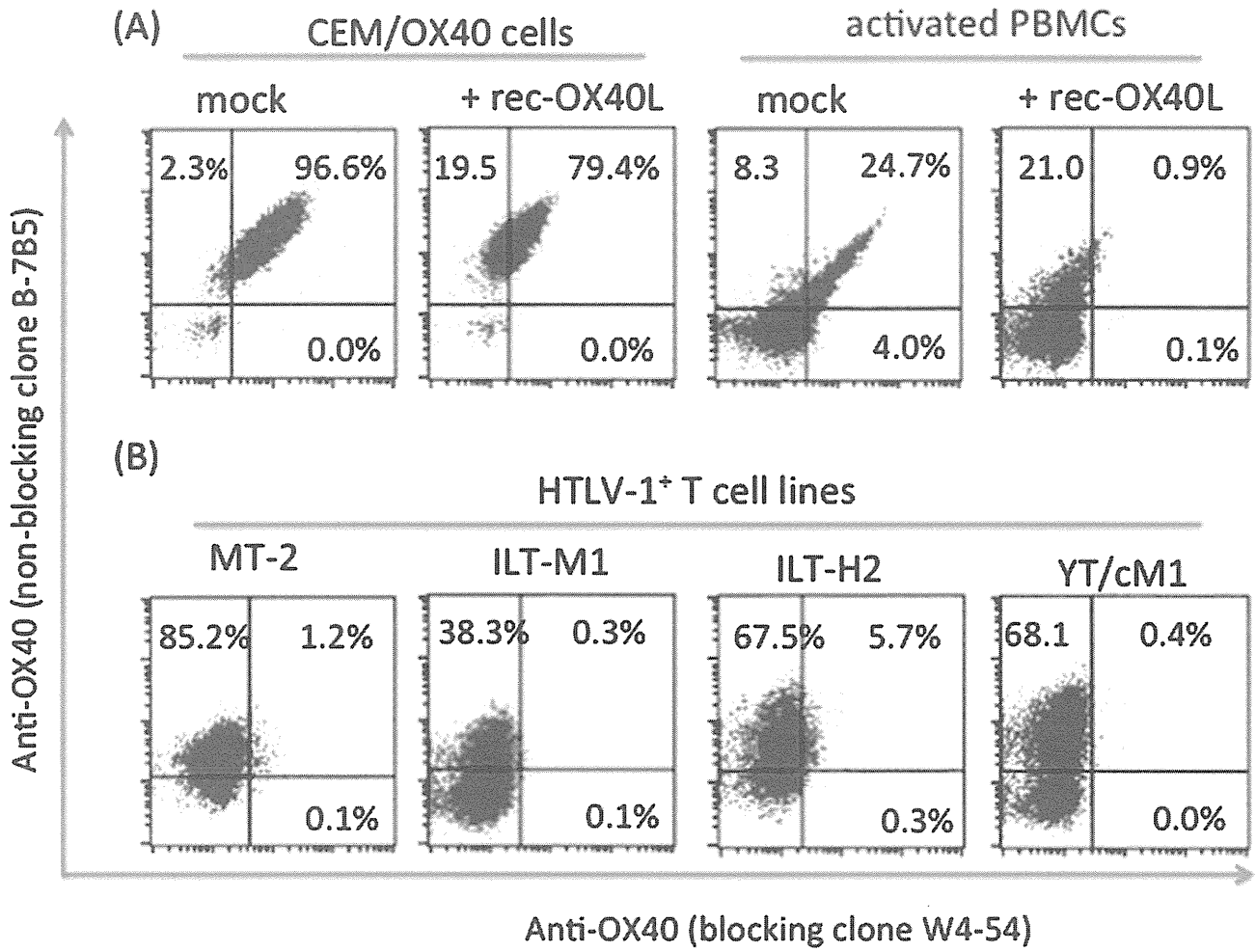

Figure 3 Blocking (clone W4-54) versus non-blocking (clone B-7B5) mAb against 2 distinct epitopes of OX40 distinguish between OX40L bound and unbound OX40. (A) OX40-expressing CEM and activated PBMCs were stained with the two mAbs in the absence (mock) or presence of 1 μg/ml of recombinant OX40L (rec-OX40L). **(B)** Various HTLV-1$^+$ T cell lines were stained with B-7B5 andW4-54 labeled with FITC and Cy5, respectively. Data shown are representative of 3 independent experiments.

OX40L-fusion proteins [28], OX40L-expressing recombinant virus [20], OX40L mRNA-transfected cells [29], lentivirus-transduced DCs [30], or autologous dying normal T cells [24]. The superiority of using cell membrane-bound OX40L as compared with the use of a soluble form was documented by data observed by the degree of inhibition of R5 HIV-1 as seen in the present study (Figure 6). These findings are in accord with a previous study that showed that the membrane-immobilized form of OX40L is highly active in the stimulation of an OX40-transfected cell line to produce cytokines [31]. In addition to OX40L, HTLV-1$^+$ cell lines may exert additional suppressing effect on R5 HIV-1 infection via Tax protein, since Tax proteins of HTLV-1 and HTLV-2 have been shown to play a role in generating antiviral responses against HIV-1 via induction of CCR5-binding chemokines *in vitro* [32]. This view is supported by the finding that co-infection with HTLV interferes with the progression of HIV-1 disease *in vivo* [33]. However, such Tax effects in the present study may be less potent than OX40L since anti-OX40L mAb significantly reversed the suppression of R5-HIV-1 induced by co-culture with autologous HTLV-1$^+$ T cell lines (Figure 5).

Conclusions

The present results demonstrate that HTLV-1$^+$ T cell line is a unique source of functional human OX40L, and suggest that autologous HTLV-1-immortalized T cell lines can be utilized as a conventional source of natural and functional OX40L in large quantities for various immunological studies.

Methods

Reagents

The medium used throughout the studies consisted of RPMI 1640 medium (Sigma-Aldrich. Inc. St. Louis, MO), supplemented with 10% fetal calf serum (FCS), 100 U/ml

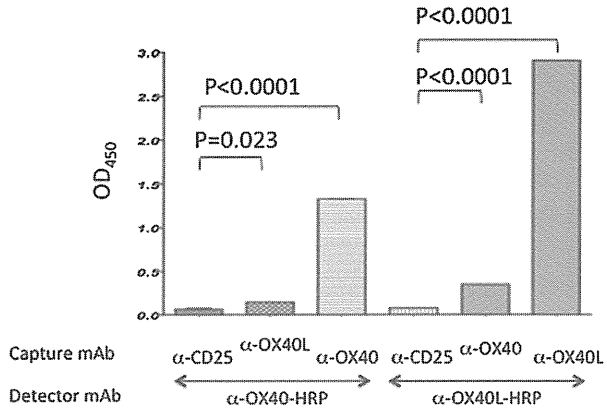

Figure 4 Presence of OX40-OX40L complexes in HTLV-1$^+$ T cell lysates. The ILT-H2 cell line derived from an ATL patient were lysed and the lysates incubated in microtiter wells that had been previously coated with either anti-CD25, OX40 or OX40L mAb for 1 hour. Anti-CD25 mAb was used as a non-specific negative control. After washing, the levels of OX40 or OX40L bound to the plates were assayed using either HRP-labeled anti-OX40 or anti-OX40L mAb. Data shown are representative of 3 independent experiments.

penicillin and 100 μg/ml streptomycin (hereinafter called RPMI medium). Anti-human CD3 mAb (clone OKT-3) and agonistic anti-CD28 mAb were purchased from the American Type Culture Collection (Rockville, MD) and Biolegend (San Diego, CA), respectively. Neutralizing mAbs against human RANTES, MIP-1α, and MIP-1β were purchased from R&D systems (Minneapolis, MN). The mouse mAbs produced in our laboratory included anti-OX40L (blocking clone 5A8 [34] and clone HD1, unpublished), anti-human OX40 (non-blocking clone B-7B5 and clone 17D8 [35]), anti-HIV-1 p24 (clones NP-24 and 2C2 [21]) and anti-CD25 (clone H-8) [36]. The rat mAbs included anti-human OX40 (blocking clone W4-54) and anti-HCV (clone Mo-8) [25,37]). Some clones were labeled with HRP using a kit (Dojin, Kumamoto, Japan) and used as the detector mAb in ELISA. These in-house mAbs were isolated from ascites fluid prepared in Balb/c or CB.17-SCID mice. The IgGs were purified utilizing a standard gel filtration method. Some of them were labeled with FITC, HiLyte Fluor 647 or Cy5 using commercial labeling kits (Dojin, GE Healthcare) according to the manufacturer's instructions. Biotinylated recombinant-soluble human OX40 (sOX40 in a form of murine IgG2a-Fc fusion protein) and OX40L (sOX40L in a form of murine CD8-fusion protein) were purchased from Ancell (Bayport, MN) and used with PE-streptavidin (BioLegend) for staining. Unlabeled glycosylated recombinant human OX40L that consists of OX40L with a human CD33 signal peptide produced in NS1 cells was purchased from R&D systems. Human recombinant IL-2 was obtained as a courtesy from the NIH-AIDS Reagent and Repository program (Bethesda, MD).

Cell lines

The HTLV-1-producing T cell lines used included the MT-2, HUT102 and the IL-2 dependent T cell lines ILT-M1 and ILT-H2 that had been generated from a HTLV-1-associated myelopathy (HAM) and an adult T cell leukemia (ATL) patient, respectively. Additional cell lines utilized included the CEM cell lines transfected with either human OX40L or OX40 (CEM/OX40L and CEM/OX40) [38]. T cells isolated from normal human donors were immortalized by HTLV-1 as follows.

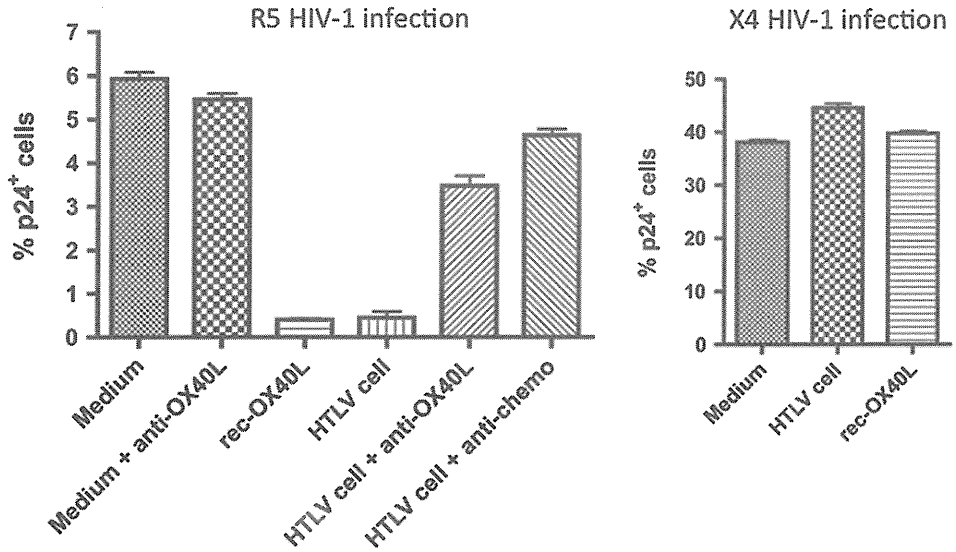

Figure 5 PFA-inactivated HTLV-1$^+$ T cells inhibit infection of activated autologous PBMCs with R5 HIV-1, but not X4 HIV-1, via OX40L and β-chemokines. In vitro activated PBMCs were infected with either R5 HIV-1 (JR-FL strain) or X4 HIV-1 (NL4-3 strain) and cultured in the presence or absence of recombinant OX40L, PFA-inactivated autologous HTLV-1$^+$ T cells, anti-OX40L blocking mAb (5A8) or a mixture of anti-β-chemokine neutralizing mAbs. After 4 days, the cells were examined for intracellular HIV-1 p24 by FCM. Data shown are representative of 3 independent experiments.

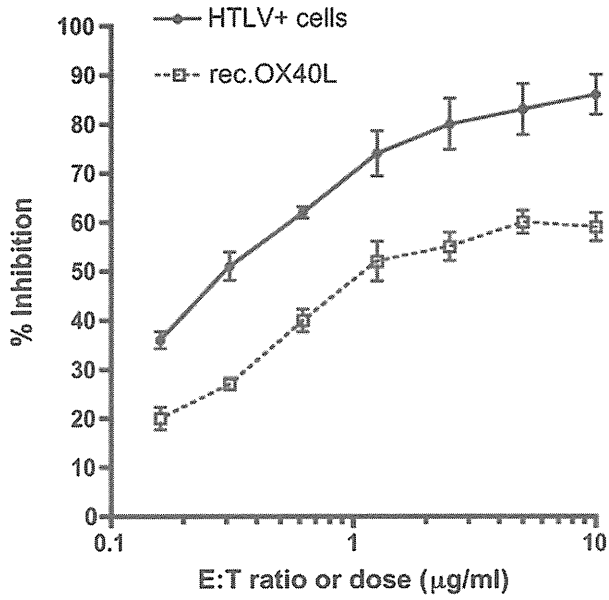

Figure 6 HTLV-1$^+$ T cells are more potent in the inhibition of R5 HIV-1 infection than recombinant soluble OX40L. R5 HIV-1-infected PBMCs prepared as in Figure 5 were cultured in the presence or absence of a graded concentration of recombinant soluble OX40L or PFA-fixed autologous HTLV-1$^+$ T cells. After 4 days, the levels of p24 produced in the culture supernatants were quantitated by ELISA. Data shown are representative of 2 independent experiments.

PBMCs from healthy donors were obtained by density gradient centrifugation of heparinized whole blood on HistoPAQUE-1077 (Sigma-Aldrich), suspended at 2 × 10^6 cells/ml in RPMI medium, dispensed into individual wells of 24-well plates (BD) (1 ml/well) pre-coated with 5 μg/ml OKT3 for 1 hour and cultured in the presence of soluble 0.1 μg/ml anti-CD28 mAb. After 24 hours at 37°C in a 5% CO_2 humidified atmosphere, the activated PBMCs were harvested and washed once. These activated PBMCs (1 × 10^6 cells/ml) were mixed with an equal number of ILT-M1 cells that were pretreated with 50 μg/ml MMC for 30 min at 37°C and cultured in RPMI media supplemented with 20 U/ml IL-2 (culture media). The cultures were performed in 24-well plates (BD) (2 ml/well) and the culture media was replenished every 3–4 days. After 1 ~ 2 months when HTLV-1 Tax$^+$ T cells appeared and started to grow continuously, they were split every 3 to 5 days using the culture medium.

Flow Cytometry (FCM)

FCM analysis of live cells was carried out as described previously. Briefly, cells to be analyzed were Fc-blocked with 2 mg/ml normal human pooled IgG on ice for 15 min. Aliquots of these cells were then subjected to staining using pre-determined optimum concentrations of fluorescent dye-conjugated mAbs for 30 min on ice. The cells were then washed using FACS buffer (PBS containing 2% FCS and 0.1% sodium azide), fixed in 1% paraformaldehyde (PFA) containing FACS buffer and analyzed using a FACS Calibur, and the data obtained were analyzed using the Cell Quest software (BD). In order to determine whether cell surface OX40 or OX40L is functional, aliquots of Fc-blocked cells were incubated with either biotinylated recombinant-OX40L (rec-OX40L) or rec-OX40 at a concentration of 2.5 μg/ml for 30 minutes on ice, followed by staining with PE-labeled streptavidin (Beckman Coulter) for 30 minutes on ice and then analyzed by FCM. For detection of HIV-1 infected cells, PBMCs were fixed with PBS containing 4% PFA followed by washing twice in FACS buffer containing 0.5% saponin. These cells were Fc-blocked with 2 mg/ml normal human pooled IgG on ice for 15 min, and aliquots of these cells were stained with FITC- or Cy5-conjugated anti-HIV-1 p24 mAb (clone 2C2) for 30 min on ice. The cells were then washed using FACS buffer and absolute cell counts of p24$^+$ cells were performed by FCM using a cell counting kit (BD) according to the manufacturer's protocol. For staining of Tax antigen, cells were fixed with PBS containing 4% PFA followed by washing in FACS buffer containing 0.5% saponin. Aliquots of these cells were stained with Cy5-conjugated mouse anti-Tax mAb (Lt-4) [39] for 30 min on ice.

ELISA and Western blot

For the quantitation of OX40L and OX40 by ELISA, anti-OX40L capture mAb (clone HD1)/ HRP-labeled detector mAb (clone 8F4) and anti-OX40 (clone B-7B5)/ HRP-labeled detector mAb (clone 17D8), respectively, were used together with recombinant standard proteins purchased from R&D systems. Immunoprecipitation followed by Western blot analysis of OX40 was performed as reported previously [40].

HIV-1 preparation and infection

HIV-$1_{JR\text{-}FL}$ and HIV-$1_{NL4\text{-}3}$ viral stocks were produced as described previously [21]. *In vitro* activated PBMCs were prepared as described above, washed once and infected with either R5 HIV-$1_{JR\text{-}FL}$ or X4 HIV-$1_{NL4\text{-}3}$ at a multiplicity of infection (m.o.i.) of 0.005 for 2 hours. After washing 3 times, PBMCs were re-suspended at 1 × 10^6 cells/ml in 20 U/ml IL-2-containing RPMI medium, dispensed into individual wells of 48-well plates (BD) (0.5 ml/well) and cultured in the presence or absence of 1 μg/ml of rec-OX40L or graded numbers of autologous HTLV-1$^+$ T cells (HTLV-1$^+$ T cells : PBMCs ratio of 10 to 0.15) that had been previously inactivated with 4% paraformaldehyde (PFA). Production of HIV-1 was determined by either the measurement of HIV-1 core p24 levels produced in the culture supernatants using our in-house formulated and standardized kits or FCM using Cy5 labeled anti-HIV-1 p24 mAb [21].

Statistical analysis

Data were tested for significance using the Student's *t* test by using Prism software (GraphPad Software).

Additional files

Additional file 1: Figure S1. Characterization of two anti-human OX40 mAbs. In the presence of B-7B5, W4-54 or isotype control mAbs, the OX40 and OX40L co-expressing control CEM cells were singly stained either with biotinylated recombinant OX40L (rec-OX40L) or rec-OX40, respectively, followed by PE-streptavidin. Data shown are representative profiles of 3 independent experiments.

Additional file 2: Figure S2. Detection of OX40 expressed by HTLV-1$^+$ T cell line (YT/cM1) by Western Blot with B-7B5 and W4-54 mAbs. Cell lysates of HTLV-1$^+$ T cell line, YT/cM1, were subjected to 10% PAGE and blotted onto nitrocellulose sheets. The sheets were then probed with anti-OX40 mAbs (B-7B5 or W4-54) or isotype controls followed by goat anti-mouse IgG or anti-rat IgG. Mol. Wt. markers are shown on the right. Data shown are representative of 2 independent experiments.

Additional file 3: Figure S3. Phenotype of HUT-102 cell line. Phenotype of HUT-102 cells were examined by FCM using anti-OX40 mAbs (FITC-labeled B-7B5 and Cy5-labeled W4-54), anti-OX40L (Cy5-labeled 5A8), biotinylated OX40 (rec-OX40) and OX40L (rec-OX40L) followed by PE-streptavidin. Intracellular Tax antigen was stained by mouse anti-Tax Lt-4 mAb.

Competing interests

The authors declare no competing financial interests.

Authors' contributions

DK and YTak generated HTLV-1$^+$ T cell lines and carried out the FCM and ELISA, performed the statistical analysis and drafted the manuscript. AT performed WB and FCM analyses. AK produced R5 and X4 HIV-1 and titrated. RT produced and labeled antibodies, confirmed their specificities and made in-house ELISA. AAA participated in the design of the study and helped to draft the manuscript. YT conceived of the study, participated in its design and coordination, carried out the HIV-1 infection experiments and drafted the manuscript. All authors read and approved the final manuscript.

Acknowledgements

This work was supported by grants from a Grant-in-Aid from the Ministry of Health, Labor and Welfare of Japan.

Author details

[1]Department of Immunology, Graduate School of Medicine, University of the Ryukyus, Okinawa 903-0215, Japan. [2]Department of Pathology, Emory University School of Medicine, Atlanta, GA 30322, USA.

Received: 10 June 2013 Accepted: 12 November 2013
Published: 18 November 2013

References

1. Ishii N, Takahashi T, Soroosh P, Sugamura K: **OX40-OX40 ligand interaction in T-cell-mediated immunity and immunopathology.** *Adv Immunol* 2010, **105**:63–98.
2. Croft M, Duan W, Choi H, Eun SY, Madireddi S, Mehta A: **TNF superfamily in inflammatory disease: translating basic insights.** *Trends Immunol* 2012, **33**:144–152.
3. Tanaka Y, Inoi T, Tozawa H, Yamamoto N, Hinuma Y: **A glycoprotein antigen detected with new monoclonal antibodies on the surface of human lymphocytes infected with human T-cell leukemia virus type-I (HTLV-I).** *Int J Cancer* 1985, **36**:549–555.
4. Miura S, Ohtani K, Numata N, Niki M, Ohbo K, Ina Y, Gojobori T, Tanaka Y, Tozawa H, Nakamura M, *et al*: **Molecular cloning and characterization of a novel glycoprotein, gp34, that is specifically induced by the human T-cell leukemia virus type I transactivator p40tax.** *Mol Cell Biol* 1991, **11**:1313–1325.
5. Ohshima Y, Tanaka Y, Tozawa H, Takahashi Y, Maliszewski C, Delespesse G: **Expression and function of OX40 ligand on human dendritic cells.** *J Immunol* 1997, **159**:3838–3848.
6. Baum PR, Gayle RB 3rd, Ramsdell F, Srinivasan S, Sorensen RA, Watson ML, Seldin MF, Clifford KN, Grabstein K, Alderson MR, *et al*: **Identification of OX40 ligand and preliminary characterization of its activities on OX40 receptor.** *Circ Shock* 1994, **44**:30–34.
7. Zingoni A, Sornasse T, Cocks BG, Tanaka Y, Santoni A, Lanier LL: **Cross-talk between activated human NK cells and CD4+ T cells via OX40-OX40 ligand interactions.** *J Immunol* 2004, **173**:3716–3724.
8. Kotani A, Hori T, Fujita T, Kambe N, Matsumura Y, Ishikawa T, Miyachi Y, Nagai K, Tanaka Y, Uchiyama T: **Involvement of OX40 ligand + mast cells in chronic GVHD after allogeneic hematopoietic stem cell transplantation.** *Bone Marrow Transplant* 2007, **39**:373–375.
9. Imura A, Hori T, Imada K, Kawamata S, Tanaka Y, Imamura S, Uchiyama T: **OX40 expressed on fresh leukemic cells from adult T-cell leukemia patients mediates cell adhesion to vascular endothelial cells: implication for the possible involvement of OX40 in leukemic cell infiltration.** *Blood* 1997, **89**:2951–2958.
10. Takasawa N, Ishii N, Higashimura N, Murata K, Tanaka Y, Nakamura M, Sasaki T, Sugamura K: **Expression of gp34 (OX40 ligand) and OX40 on human T cell clones.** *Jpn J Cancer Res* 2001, **92**:377–382.
11. Kondo K, Okuma K, Tanaka R, Zhang LF, Kodama A, Takahashi Y, Yamamoto N, Ansari AA, Tanaka Y: **Requirements for the functional expression of OX40 ligand on human activated CD4+ and CD8+ T cells.** *Hum Immunol* 2007, **68**:563–571.
12. Croft M: **Control of immunity by the TNFR-related molecule OX40 (CD134).** *Annu Rev Immunol* 2010, **28**:57–78.
13. Latza U, Durkop H, Schnittger S, Ringeling J, Eitelbach F, Hummel M, Fonatsch C, Stein H: **The human OX40 homolog: cDNA structure, expression and chromosomal assignment of the ACT35 antigen.** *Eur J Immunol* 1994, **24**:677–683.
14. Baum PR, Gayle RB 3rd, Ramsdell F, Srinivasan S, Sorensen RA, Watson ML, Seldin MF, Baker E, Sutherland GR, Clifford KN, *et al*: **Molecular characterization of murine and human OX40/OX40 ligand systems: identification of a human OX40 ligand as the HTLV-1-regulated protein gp34.** *EMBO J* 1994, **13**:3992–4001.
15. Weinberg AD, Evans DE, Thalhofer C, Shi T, Prell RA: **The generation of T cell memory: a review describing the molecular and cellular events following OX40 (CD134) engagement.** *J Leukoc Biol* 2004, **75**:962–972.
16. Compaan DM, Hymowitz SG: **The crystal structure of the costimulatory OX40-OX40L complex.** *Structure* 2006, **14**:1321–1330.
17. Imura A, Hori T, Imada K, Ishikawa T, Tanaka Y, Maeda M, Imamura S, Uchiyama T: **The human OX40/gp34 system directly mediates adhesion of activated T cells to vascular endothelial cells.** *J Exp Med* 1996, **183**:2185–2195.
18. Weinberg AD: **OX40: targeted immunotherapy–implications for tempering autoimmunity and enhancing vaccines.** *Trends Immunol* 2002, **23**:102–109.
19. Croft M, So T, Duan W, Soroosh P: **The significance of OX40 and OX40L to T-cell biology and immune disease.** *Immunol Rev* 2009, **229**:173–191.
20. Liu J, Ngai N, Stone GW, Yue FY, Ostrowski MA: **The adjuvancy of OX40 ligand (CD252) on an HIV-1 canarypox vaccine.** *Vaccine* 2009, **27**:5077–5084.
21. Tanaka R, Takahashi Y, Kodama A, Saito M, Ansari AA, Tanaka Y: **Suppression of CCR5-tropic HIV type 1 infection by OX40 stimulation via enhanced production of beta-chemokines.** *AIDS Res Hum Retroviruses* 2010, **26**:1147–1154.
22. Higashimura N, Takasawa N, Tanaka Y, Nakamura M, Sugamura K: **Induction of OX40, a receptor of gp34, on T cells by trans-acting transcriptional activator, Tax, of human T-cell leukemia virus type I.** *Jpn J Cancer Res* 1996, **87**:227–231.
23. Pichler K, Kattan T, Gentzsch J, Kress AK, Taylor GP, Bangham CR, Grassmann R: **Strong induction of 4-1BB, a growth and survival promoting costimulatory receptor, in HTLV-1-infected cultured and patients' T cells by the viral tax oncoprotein.** *Blood* 2008, **111**:4741–4751.
24. Kondo K, Okuma K, Tanaka R, Matsuzaki G, Ansari AA, Tanaka Y: **Rapid induction of OX40 ligand on primary T cells activated under DNA-damaging conditions.** *Hum Immunol* 2008, **69**:533–542.
25. Baba E, Takahashi Y, Lichtenfeld J, Tanaka R, Yoshida A, Sugamura K, Yamamoto N, Tanaka Y: **Functional CD4 T cells after intercellular molecular transfer of 0X40 ligand.** *J Immunol* 2001, **167**:875–883.

26. Nam KO, Kang H, Shin SM, Cho KH, Kwon B, Kwon BS, Kim SJ, Lee HW: **Cross-linking of 4-1BB activates TCR-signaling pathways in CD8+ T lymphocytes.** *J Immunol* 2005, **174**:1898–1905.
27. Ma BY, Mikolajczak SA, Danesh A, Hosiawa KA, Cameron CM, Takaori-Kondo A, Uchiyama T, Kelvin DJ, Ochi A: **The expression and the regulatory role of OX40 and 4-1BB heterodimer in activated human T cells.** *Blood* 2005, **106**:2002–2010.
28. Taylor L, Bachler M, Duncan I, Keen S, Fallon R, Mair C, McDonald TT, Schwarz H: **In vitro and in vivo activities of OX40 (CD134)-IgG fusion protein isoforms with different levels of immune-effector functions.** *J Leukoc Biol* 2002, **72**:522–529.
29. Dannull J, Nair S, Su Z, Boczkowski D, DeBeck C, Yang B, Gilboa E, Vieweg J: **Enhancing the immunostimulatory function of dendritic cells by transfection with mRNA encoding OX40 ligand.** *Blood* 2005, **105**:3206–3213.
30. Tateyama M, Fujihara K, Ishii N, Sugamura K, Onodera Y, Itoyama Y: **Expression of OX40 in muscles of polymyositis and granulomatous myopathy.** *J Neurol Sci* 2002, **194**:29–34.
31. Muller N, Wyzgol A, Munkel S, Pfizenmaier K, Wajant H: **Activity of soluble OX40 ligand is enhanced by oligomerization and cell surface immobilization.** *FEBS J* 2008, **275**:2296–2304.
32. Barrios CS, Castillo L, Giam CZ, Wu L, Beilke MA: **Inhibition of HIV Type 1 replication by human T lymphotropic virus Types 1 and 2 Tax Proteins in Vitro.** *AIDS Res Hum Retroviruses* 2013, **29**:1061–1067.
33. Beilke MA: **Retroviral coinfections: HIV and HTLV: taking stock of more than a quarter century of research.** *AIDS Res Hum Retroviruses* 2012, **28**:139–147.
34. Tozawa H, Andoh S, Takayama Y, Tanaka Y, Lee B, Nakamura H, Hayami M, Hinuma Y: **Species-dependent antigenicity of the 34-kDa glycoprotein found on the membrane of various primate lymphocytes transformed by human T-cell leukemia virus type-I (HTLV-I) and simian T-cell leukemia virus (STLV-I).** *Int J Cancer* 1988, **41**:231–238.
35. Takahashi Y, Tanaka R, Yamamoto N, Tanaka Y: **Enhancement of OX40-induced apoptosis by TNF coactivation in OX40-expressing T cell lines in vitro leading to decreased targets for HIV type 1 production.** *AIDS Res Hum Retroviruses* 2008, **24**:423–435.
36. Tanaka Y, Inoi T, Tozawa H, Sugamura K, Hinuma Y: **New monoclonal antibodies that define multiple epitopes and a human-specific marker on the interleukin 2 receptor molecules of primates.** *Microbiol Immunol* 1986, **30**:373–388.
37. Inudoh M, Kato N, Tanaka Y: **New monoclonal antibodies against a recombinant second envelope protein of Hepatitis C virus.** *Microbiol Immunol* 1998, **42**:875–877.
38. Takahashi Y, Tanaka Y, Yamashita A, Koyanagi Y, Nakamura M, Yamamoto N: **OX40 stimulation by gp34/OX40 ligand enhances productive human immunodeficiency virus type 1 infection.** *J Virol* 2001, **75**:6748–6757.
39. Lee B, Tanaka Y, Tozawa H: **Monoclonal antibody defining tax protein of human T-cell leukemia virus type-I.** *Tohoku J Exp Med* 1989, **157**:1–11.
40. Tanaka R, Yoshida A, Murakami T, Baba E, Lichtenfeld J, Omori T, Kimura T, Tsurutani N, Fujii N, Wang ZX, *et al*: **Unique monoclonal antibody recognizing the third extracellular loop of CXCR4 induces lymphocyte agglutination and enhances human immunodeficiency virus type 1-mediated syncytium formation and productive infection.** *J Virol* 2001, **75**:11534–11543.

doi:10.1186/1743-422X-10-338
Cite this article as: Kasahara *et al.*: Natural OX40L expressed on human T cell leukemia virus type-I-immortalized T cell lines interferes with infection of activated peripheral blood mononuclear cells by CCR5-utilizing human immunodeficiency virus. *Virology Journal* 2013 **10**:338.

AIDS RESEARCH AND HUMAN RETROVIRUSES
Volume 29, Number 00, 2013

DOI: 10.1089/aid.2013.0109

Genes Related to Antiviral Activity, Cell Migration, and Lysis Are Differentially Expressed in CD4$^+$ T Cells in Human T Cell Leukemia Virus Type 1-Associated Myelopathy/Tropical Spastic Paraparesis Patients

Mariana Tomazini Pinto,[1,2] Tathiane Maistro Malta,[1,2] Evandra Strazza Rodrigues,[1,2] Daniel Guariz Pinheiro,[1,3] Rodrigo Alexandre Panepucci,[1,4] Kelen Cristina Ribeiro Malmegrim de Farias,[1,2] Alessandra De Paula Sousa,[1] Osvaldo Massaiti Takayanagui,[4] Yuetsu Tanaka,[5] Dimas Tadeu Covas,[1,4] and Simone Kashima[1,2]

Abstract

Human T cell leukemia virus type 1 (HTLV-1) preferentially infects CD4$^+$ T cells and these cells play a central role in HTLV-1 infection. In this study, we investigated the global gene expression profile of circulating CD4$^+$ T cells from the distinct clinical status of HTLV-1-infected individuals in regard to TAX expression levels. CD4$^+$ T cells were isolated from asymptomatic HTLV-1 carrier (HAC) and HTLV-1-associated myelopathy/tropical spastic paraparesis (HAM/TSP) patients in order to identify genes involved in HAM/TSP development using a microarray technique. Hierarchical clustering analysis showed that healthy control (CT) and HTLV-1-infected samples clustered separately. We also observed that the HAC and HAM/TSP groups clustered separately regardless of TAX expression. The gene expression profile of CD4$^+$ T cells was compared among the CT, HAC, and HAM/TSP groups. The paxillin (*Pxn*), chemokine (C-X-C motif) receptor 4 (*Cxcr4*), interleukin 27 (*IL27*), and granzyme A (*Gzma*) genes were differentially expressed between the HAC and HAM/TSP groups, regardless of TAX expression. The perforin 1 (*Prf1*) and forkhead box P3 (*Foxp3*) genes were increased in the HAM/TSP group and presented a positive correlation to the expression of TAX and the proviral load (PVL). The frequency of CD4$^+$FOXP3$^+$ regulatory T cells (Treg) was higher in HTLV-1-infected individuals. *Foxp3* gene expression was positively correlated with cell lysis-related genes (*Gzma*, *Gzmb*, and *Prf1*). These findings suggest that CD4$^+$ T cell activity is distinct between the HAC and HAM/TSP groups.

Introduction

HUMAN T CELL LEUKEMIA VIRUS type 1 (HTLV-1) was the first human retrovirus isolated.[1] HTLV-1 is the etiologic agent of HTLV-1-associated myelopathy/tropical spastic paraparesis (HAM/TSP),[2,3] adult T cell leukemia/lymphoma (ATLL),[4,5] and several inflammatory diseases including polymyositis, arthropathy, infective dermatitis, uveitis, and Sjögren's syndrome.[6–10]

The disease manifestations occur in 2–5% of infected individuals, and most individuals remain asymptomatic throughout life.[11,12] The mechanisms that lead to disease in infected patients are not fully understood and a number of factors such as genetic, demographic, environmental, and others have been suggested to contribute to disease development.[13–15]

HAM/TSP is a chronic progressive inflammatory disorder of the central nervous system (CNS) characterized by slow progressive spastic paraparesis, bladder disorder, weakness of the lower limbs, and less conspicuous sensory signs.[16] The clinical course of HAM/TSP varies among patients, but is more common in females.[17–19] Among several HTLV-1 genes, a transcriptional activator *Tax* may play a major role in the development of HAM/TSP, regulating multiple cellular responses by protein–protein interactions with various host cell factors. Moreover, *Tax* has been

[1]National Institute of Science and Technology in Stem Cell and Cell Therapy, Center for Cell-Based Therapy and Regional Blood Center of Ribeirão Preto, Ribeirão Preto, Brazil.
[2]Faculty of Pharmaceutical Sciences, University of São Paulo, Ribeirão Preto, Brazil.
[3]Department of Genetics, Faculty of Medicine of Ribeirão Preto, University of São Paulo, Ribeirão Preto, Brazil.
[4]Faculty of Medicine of Ribeirão Preto, University of São Paulo, Ribeirão Preto, Brazil.
[5]Department of Immunology, Graduate School of Medicine, University of the Ryukyus, Okinawa, Japan.

shown to disrupt cell cycle and DNA repair checkpoint, inactivate several tumor suppressors, and stimulate cell growth, while protecting against apoptosis.[20,21]

Although HTLV-1 is known to infect a wide range of human and nonhuman cells *in vitro*, HTLV-1 preferentially infects CD4 T cells, which become the main reservoir of HTLV-1.[22] It is also known that CD4 T cells predominate in the spinal cord mononuclear infiltrate of HAM/TSP patients.[23] In this way, in the early stages of the inflammatory process, cytokines such as interleukin (IL)-1α, tumor necrosis factor (TNF)-α, and interferon (IFN)-γ are spontaneously secreted by these cells.[24] Thus, the potential contribution of CD4 T cells to the pathogenesis of this inflammatory disease as well as their expansion in HAM/TSP is more efficient due to the chronic antigenic stimulation that occurs in these individuals.[25,26]

The aim of this work was to identify genes differentially expressed among healthy control (CT), asymptomatic HTLV-1 carrier (HAC), and HAM/TSP patients in $CD4^+$ T cells isolated from these individuals. We showed that the global gene expression profile of circulating $CD4^+$ T cells from HTLV-1 individuals harboring distinct clinical status was altered regardless of TAX expression levels. Considering that most HTLV-1-infected individuals remain asymptomatic throughout life we explored genes that could be involved with HAM/TSP development.

Materials and Methods

HTLV-1-infected individuals and healthy controls

A total of 47 peripheral whole blood samples from HTLV-1-infected individuals were obtained and divided into two groups: the asymptomatic HAC group comprised of 26 individuals and the HAM/TSP group comprised of 21 symptomatic patients. Healthy controls (CT; $n=28$) had no previous or current infectious diseases caused by blood-borne pathogens. Samples of the CT individuals were recruited from the Regional Blood Center of Ribeirão Preto, São Paulo, Brazil, and HTLV-1-infected individuals were recruited from the Neurology Department of the Clinical Hospital of the Medical School of the University of São Paulo, Ribeirão Preto, São Paulo, Brazil.

The study was approved by the Institutional Ethics Committee (process number 3083/2007) and all individuals signed an informed consent before enrollment. All HTLV-1-infected individuals were evaluated for clinical status according to the criteria previously described for ATLL and HAM/TSP.[27] To be included in this study, the HTLV-1-infected individuals must have serological (rp21e-enhanced EIA; Cambridge Biotech) and molecular [conventional long-term repeat (LTR) and TAX polymerase chain reaction (PCR)] confirmation of the HTLV-1 infection.

All HTLV-1-infected and CT individuals included in this study presented negative serology for other relevant blood-borne pathogens including hepatitis B virus, hepatitis C virus, human immunodeficiency virus, Chagas disease, and syphilis. Hemogram and CD4 and CD8 T cell counts were performed for all individuals.

Molecular diagnosis and proviral load

Genomic DNA was extracted using the Super Quick Gene DNA isolation kit (Analytical Genetic Testing Center–AGTC, Denver, CO) following the manufacturer's instructions. The in house PCR (LTR and Tax regions) tests were as previously described.[28] The proviral load was quantified using TaqMan Universal PCR Master Mix (Applied Biosystems, Foster City, CA) and specific primers of the HTLV-1 Tax region. The reaction was composed of 500 ng of genomic DNA, 6.25 μl TaqMan Universal PCR Master Mix, 5 μM of the forward primer (5'-CCC ATC GAT GGA CGC GT-3'), 5 μM of the reverse primer (5'-CTC CTT CCC CAC CCA GAG AA-3'), and 5 μM of the specific probe (5'-FAM-CGG CTC AGC TCT ACA G-3'-MGB). Human β-actin (*Actb*) was used as the endogenous control (TaqMan Gene Expression Assays–Hs03023880_g1) (Applied Biosystems, Foster City, CA). Serially diluted (from 10^5 to 10^1 copies) DNA from HTLV-1-infected MT-2 cells was used for generating standard curves for the HTLV-1 *Tax* gene. Real-time PCR was performed in duplicate for all DNA standards and samples using the ABI Prism 7500 Sequence Detection System (Applied Biosystems, Foster City, CA) with the following conditions: 50°C for 2 min, 95°C for 10 min, followed by 40 cycles at 95°C for 15 s/60°C for 1 min. Proviral load was calculated using the following formula: (copy number of *Tax*)/(copy number of β-actin)$\times 2 \times 100{,}000$.

$CD4^+$ T cell isolation

Peripheral blood mononuclear cells (PBMCs) were isolated by Ficoll Hypaque PLUS (GE Healthcare Bio-Sciences AB, Uppsala, Sweden). $CD4^+$ T cells were then isolated from PBMCs by positive selection using immunomagnetic beads (Miltenyi Biotec GmbH, Bergisch Gladbach, Germany) and the purity of the $CD3^+CD4^+$ T cells was confirmed by flow cytometry using the surface markers anti-CD4-FITC and anti-CD3-PE (FACSCalibur, Becton & Dickinson, San Jose, CA).

Microarray analysis

Twelve samples underwent microarray analysis, as follows: four CT, four HAC, and four HAM/TSP samples. The criterion used to select HTLV-1-infected individuals was TAX expression levels in PBMCs as assessed by flow cytometry. Two samples had high TAX expression and two samples had low TAX expression for both groups (Table 1). All samples had purity above 90%. We considered high TAX expression levels those with values higher than 1.39% (obtained by the median of all HTLV-1-infected individuals). In these samples, proviral load correlated with TAX expression (data not shown). Total RNA was isolated with *TRIzol Reagent* (Invitrogen, Carlsbad, CC) and purified with the RNeasy Mini Kit (Qiagen, Hilden, Germany).

One color microarray-based gene expression analysis (Quick Amp Labeling) (Agilent, Santa Clara, CA) was done according to the manufacturer's instructions. The microarray was scanned with an Axon GenePix 4000B Microarray Scanner (Molecular Devices, Sunnyvale, CA) and data were processed using Feature Extraction software version 9.5.1 (Agilent, Santa Clara, CA). Quality control and array normalization were done in R environment at (www.r-project.org) with the Agi4x44PreProcess bioconductor package (http://bioconductor.org/). Normalization and filtering were done following the Agi4x44-Pre-Process instructions. Genes differentially expressed were identified based on a $\log_2$-fold change of 2-fold at least and a statistically significant level using the *t*-test (p value < 0.005). The expression profiles of the differentially expressed genes were determined by cluster analysis based on the k-means method using Euclidean distance (Genesis 1.7.5). Ingenuity

TABLE 1. DESCRIPTIVE CHARACTERISTICS OF HUMAN T CELL LEUKEMIA VIRUS TYPE 1-INFECTED INDIVIDUALS INCLUDED IN THE MICROARRAY ANALYSIS

Clinical status	*Gender*	*Age (years)*	*TAX expression in CD4$^+$ (%)*	*Leukocytes global count (cells/mm^3)*	*Absolute count of CD4/CD8 (reason)*	*Purity (%) CD4$^+$*
HAC 08	F	26	8.87	5,600	1251/760 (1.65)	96.87
HAC 16	F	55	0.14	7,100	708/237 (2.98)	95.22
HAC 19	F	33	0.16	4,800	1166/274 (4.26)	95.02
HAC 21	M	46	3.32	6,700	1225/558 (2.20)	95.31
HAM 01	F	55	0.44	6,000	717/378 (1.90)	94.94
HAM 09	M	64	3.66	3,700	468/355 (1.32)	96.31
HAM 14	F	61	2.97	6,000	665/256 (2.60)	93.82
HAM 17	F	55	0.54	8,600	579/272 (2.13)	93.62

Characteristics according to gender, age, TAX expression in CD4$^+$ T cells, leukocyte global count, absolute count of CD4/CD8, and purity of CD4$^+$ T cells.

HTLV-1, human T cell leukemia virus type 1; HAC, asymptomatic HTLV-1 carrier; HAM/TSP, HTLV-1-associated myelopathy/tropical spastic paraparesis; F, female; M, male.

Pathway Analysis (IPA) was used to evaluate the microarray data for relevant biological themes within the differentially expressed genes. Microarray data have been deposited in the NCBI Gene Expression Omnibus (www.ncbi.nlm.nih.gov/geo/) (GEO ID: GSE38537).

Real-Time RT-PCR

Total RNA was reverse transcribed (RT) using the High Capacity cDNA Reverse Transcription Kit (Applied Biosystems, Foster City, CA) following the manufacturer's instructions. Differentially expressed genes were validated by a real-time PCR technique using TaqMan Gene Expression Assays (Applied Biosystems, Foster City, CA). The PCR amplification and fluorescence data collection were performed with ABI 7500 Sequence Detection (Applied Biosystems, Foster City, CA).

The following genes were validated: granzyme A (*Gzma*) (Hs00196206_m1), granzyme B (*Gzmb*) (Hs00188051_m1), perforin 1 (*Prf1*) (Hs00169473_m1), chemokine (C-X-C motif) receptor 4 (*Cxcr4*) (Hs00237052_m1), paxillin (*Pxn*) (Hs01104424_m1), forkhead box P3 (*Foxp3*) (Hs01085834_m1), and interleukin 27 (*IL27*) (Hs00377366_m1).

The housekeeping genes β-actin (*Actb*) (4326315E), glyceraldehyde-3-phosphate dehydrogenase (*Gapdh*) (4310884-E), β_2-microglobulin (*B2m*) (4333766-0710013), and ribosomal protein L13a (*Rpl13a*) (185720330-7)[29] were used to normalize sample loading (Applied Biosystems). The $2^{-\Delta\Delta Ct}$ method was used to calculate the relative expression levels.[30] All the reactions were duplicated.

Flow cytometry analysis

TAX expression was detected in PBMCs. Cells were cultured in RPMI 1640 (Sigma-Aldrich, Saint Louis, MO) containing 10% fetal calf serum (HyClone, Logan, UT) and 20 nM concanamycin A (Sigma-Aldrich, St. Louis, MO) for 12 h under 5% CO_2 at 37°C.

A total of 2.5×10^5 cells were stained for surface markers anti-CD4-PE, anti-CD8-PerCP, and anti-CD3-APC (Becton & Dickinson, San Jose, CA). For intracellular analysis, cells were fixed with 4% paraformaldehyde in phosphate-buffered saline (PBS) for 20 min.

Fixed cells were washed with PBS containing 4% normal goat serum (NGS) (Sigma) and then washed with PBS containing 0.1% Triton X-100 (Sigma) for 10 min at room temperature. Permeabilized cells were washed and resuspended in PBS/4% NGS containing an anti-HTLV-I TAX monoclonal antibody (mAb) (Lt-4; IgG_3), antihuman-PRF1-clone δG9, antihuman-GZMB-clone GB11 (Becton & Dickinson, San Jose, CA), or an isotype control mAb (Southern Biotechnology Associates, Birmingham, AL) for 30 min at room temperature. For intracellular TAX detection, cells were stained with Alexa Fluor 488-labeled goat antimouse IgG_3 (Invitrogen, Carlsbad, CA) for 30 min at room temperature.

For CXCR4 detection, 150 μl of whole blood and 5 μl of antibodies anti-CD4-FITC, anti-CD3-PerCP, and anti-human-CXCR4-PE-clone 12G5 (Becton & Dickinson, San Jose, CA) were used. The reaction was incubated for 15 min and then 1 ml of FACS Lysing Solution (1×) (Becton & Dickinson, San Jose, CA) was added. All samples were analyzed on a FACSCalibur flow cytometer (Becton & Dickinson, San Jose, CA).

For FOXP3 expression, isolated PBMCs were immunostained with a saturating concentration of anti-CD25-FITC, anti-CD4-PerCP, and anti-CD3-APC for 15 min at room temperature. Then 1 ml of FACS Lysing Solution (1×) (Becton & Dickinson, San Jose, CA) was added. Cells were permeabilized using FACS Permeabilizing Solution 2 (Becton & Dickinson, San Jose, CA) and stained intracellularly for 10 min with antihuman-FOXP3-PE-clone 259/C7. Finally, the cells were washed with PBS and analyzed on a FACSCalibur flow cytometer (Becton & Dickinson, San Jose, CA).

Statistical analysis

Data were analyzed in GraphPad PRISM, version 5.01 (GraphPad software California) using nonparametric statistical tests. The results from quantitative PCR and flow cytometry were analyzed using a one-tailed Mann–Whitney *U*-test. The correlations among different parameters were assessed with Spearman's rank correlation. In all these cases, statistically significant differences were considered when p values were ≤ 0.05.

Results

Clinical and demographic data

The clinical and demographic data of patients are shown in Table 2. A total of 75 individuals were included in our study of

Table 2. Clinical and Viral Characteristics of Human T Cell Leukemia Virus Type 1-Infected Individuals and Healthy Controls Enrolled in the Study

	CT (n=*28*)	*HAC* (n=*26*)	*HAM/TSP* (n=*21*)
Age	46.5	42.9	54.9
Gender (F:M)	2.5	1.4	3.2
Proviral load mean (copy number/10^5 cells)[a]	—	6,586	12,233[b]
TAX expression (%)	—	1.1	2.5[b]
Leukocyte global count (cells/mm^3)	7,225	6,816	6,771
CD4/CD8 ratio	2.21	2.10	2.98

[a]Proviral load copy number/10^5 cells.
[b]$p \leq 0.01$ (unpaired t test).
Table shows average values. CT, healthy controls; HAC, asymptomatic HTLV-1 carrier; HAM/TSP, HTLV-1-associated myelopathy/tropical spastic paraparesis; F:M, female/male ratio.

which 51 were female (68%). The mean onset age in the HAM/TSP group was 54.9 years (ranging from 37 to 74 years), which was higher than the CT (mean 46.5 years) and HAC groups (mean onset age 42.9 years). Proviral load was increased (1.8×) in the HAM/TSP group ($p=0.0024$) when compared to the HAC group (data not shown). TAX expression positively correlated with proviral load ($r=0.7433$; $p<0.0001$) and the percentage of $CD4^+$ T cells expressing TAX was higher in the HAM/TSP group (data not shown). No differences were observed in leukocyte global counts and CD4/CD8 ratio among groups.

Global gene expression in $CD4^+$ T cells

The microarray platform was tested with 12 individual samples divided according to patients' clinical status and TAX expression as follows: CT ($n=4$), HAC ($n=4$; composed of two samples with high TAX expression and two with low TAX expression), and HAM/TSP group ($n=4$; composed of two samples with high TAX expression and two with low TAX expression). We used a hierarchical clustering to group samples according to their gene expression levels. Dendrogram analysis showed that clustering of $CD4^+$ T cells allowed a clear separation between CT and HTLV-1-infected individuals. We also observed that the HAC and HAM/TSP groups clustered apart (Fig. 1). However, HTLV-1 $CD4^+$ T cell clustering did not correlate with TAX protein expression.

Gene expression analysis

A total of 45,015 probes were screened by the Agilent microarray platform. The background correction, filtering, normalization, and summarization of probes were performed using the Agi4x44PreProcess package resulting in 27,061 distinct probes, from which only 19,668 remained in the subsequent analysis after the filtering of probes annotated as ribosomal proteins, or in sexual chromosomes or unannotated probes. In microarray analysis, genes were considered differentially expressed on the basis of a $\log_2$-fold change of 2-fold at least and a statistically significant level using a t-test (p value < 0.005). We found 201 differently expressed genes between the CT and HAC groups (166 genes down-regulated and 35 genes up-regulated in the HAC group), 244 genes between the CT and HAM/TSP groups (165 genes down-regulated and 79 genes up-regulated in the HAM/TSP group), and 68 genes between the HAC and HAM/TSP groups (66 genes down-regulated and 2 genes up-regulated in the HAM/TSP group) (Fig. 2A–C). Additionally, we determined which genes were in common among these groups (Fig. 2D). Supplementary Tables S1–S6 (Supplementary Data are available online at www.liebertpub.com/aid) SUPPL TABLES S1–S6 list all genes shown in Venn diagrams. Only one differentially expressed gene (*Tmeff2*) was observed between HAM/TSP vs. HAC and CT vs. HAC analysis. We did not select this gene to study because it was not associated with inflammatory and infectious disease.

Genes related to cell migration were up-regulated in the HAM/TSP group

Eighty-four differentially expressed genes in common were observed between CT vs. HAC and CT vs. HAM/TSP analysis, with most of them overexpressed in the CT group (Fig. 3A). *In silico* analysis demonstrated that six genes, namely paxillin (*Pxn*), CD4, *Ptk2b*, *Ccl5*, *Tnf*, and *Gh1*, were represented in a network that is related to apoptosis, inflammatory and immunological diseases, cell–cell interaction, movement and repair of cell functions, and cell migration (Fig. 3B). The *Pxn* gene was also present in the *Cxcr4* pathway that is responsible for cell migration. The global gene expression profile showed that *Pxn* was increased in the CT group compared to the HAC (fold change: 5.1, $p=0.0913$) and HAM/TSP groups (fold change: 8.2, $p=0.0002$). The *Pxn* and *Cxcr4* genes were validated by quantitative real-time PCR (qPCR) and both of them showed an increased expression in HAM/TSP individuals (Fig. 3C). The level of *Pxn* gene expression was increased in HTLV-1-infected individuals ($p=0.0022$) (data not shown). Moreover, the CXCR4 protein was analyzed by flow cytometry among the groups, but no statistically significant difference was observed (data not shown).

IL27 gene expression is higher in HAC individuals

Forty-two differentially expressed genes exclusive between HAC and HAM/TSP analysis were found. These genes were related to cell–cell interaction, inflammatory response, and cellular immune response, which include interleukin 27 (*IL27*). A global gene expression profile showed that *IL27* was increased in the HAC group compared to the HAM/TSP groups (fold change: 5.24). This result was validated by qPCR in which levels of *IL27* gene expression were higher in the HAC group compared to the HAM/TSP group ($p=0.0392$) (Fig. 4A). Additionally, *IL27* gene expression was higher in HTLV-1-infected individuals compared to the CT group ($p=0.0019$) (data not shown).

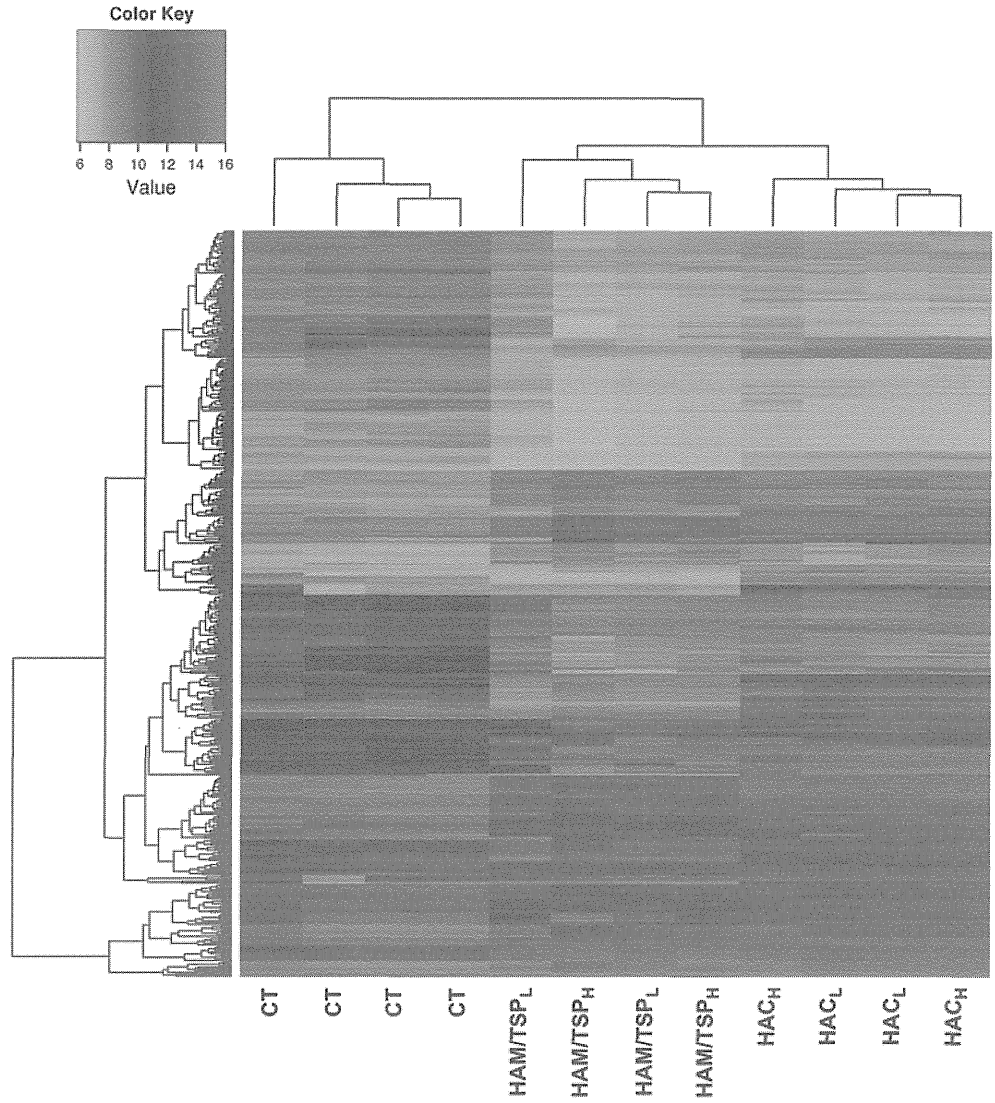

FIG. 1. Gene expression heat map and dendrogram of CD4$^+$ T cells. Hierarchical clustering of all detected genes showed a clear clustering of CT, HAC, and HAM/TSP samples using an average linkage and Euclidian distance metric. Expression values from all microarrays were used to group transcription profiles according to their similarities among groups. The heat map shows a distinct gene expression profile in the three groups analyzed. Rows indicate the relative levels of expression for a single gene, and columns show the expression level for a single sample. Green and red colors indicate those genes with lower and higher expression levels, respectively. CT, healthy control; HAC, asymptomatic human T cell leukemia virus type 1 (HTLV-1) carrier; HAM/TSP, HTLV-1-associated myelopathy/tropical spastic paraparesis; HAC$_L$, low TAX expression; HAC$_H$, high TAX expression; HAM/TSP$_L$, low TAX expression; HAM/TSP$_H$, high TAX expression.

HAM/TSP CD4$^+$ T cells had higher expression of cell lysis-related genes

The 25 differentially expressed genes in common between CT vs. HAM/TSP and HAM/TSP vs. HAC analyses were evaluated for their participation in signaling pathways and only three pathways were observed, among them granzyme A (*Gzma*). Although the *Gzma* gene was not in accordance with the parameters of analyses (2-fold and p value 0.005), the global gene expression profile showed that *Gzma* was increased in the HAM/TSP group compared to the CT (fold change: 1.9, $p=0.0038$) and HAC groups (fold change: 1.9, $p=0.0071$). For that reason, this gene was selected for validation due to it being poorly studied on CD4$^+$ T cells infected by HTLV-1 and due to its possible involvement in HAM/TSP development.

The levels of *Gzma* gene expression were evaluated (Fig. 4B) and we observed an increase in the HAM/TSP group compared to the CT ($p=0.0038$) and HAC ($p=0.0071$) groups. Therefore, we suggest that other genes related to cell lysis could also be increased in the HAM/TSP group, such as *Gzmb* and *Prf1*. Therefore, we analyzed *Gzmb* and *Prf1* gene expression (Fig. 4C and D). The HAM/TSP group showed higher gene expression levels of *Prf1* compared to the CT ($p<0.0001$) and HAC ($p=0.0037$) groups. *Prf1* gene expression was increased ($p=0.003$) in HTLV-1-infected individuals when compared to the CT group (data not shown). No difference was observed in gene expression level of *Gzmb* among the three groups. GZMB and PRF1 proteins were analyzed by flow cytometry; however, no difference was observed among the CT, HAC, and HAM/TSP groups (data not shown).

It was reported that regulatory T cells (Treg) have cytolytic capacity and perforin/granzyme pathways are required for this activity.[31] *Foxp3* gene expression, one of the main Treg cell markers, was also evaluated (Fig. 4E). As expected, we notice an overexpression of *Foxp3* in the HAM/TSP group compared to the CT and HAC groups ($p=0.0003$ and $p=0.0016$, respectively). *Foxp3* gene expression was increased in HTLV-1-infected individuals ($p=0.0128$) compared to CT individuals (data not shown).

The lysis-related genes were correlated with Foxp3 expression and Prf1 and Foxp3 genes were correlated with TAX expression and proviral load (PVL)

Since the *Gzma*, *Prf1*, and *Foxp3* genes were shown to have an increased expression in HAM/TSP individuals, we thought these genes could be correlated. We performed

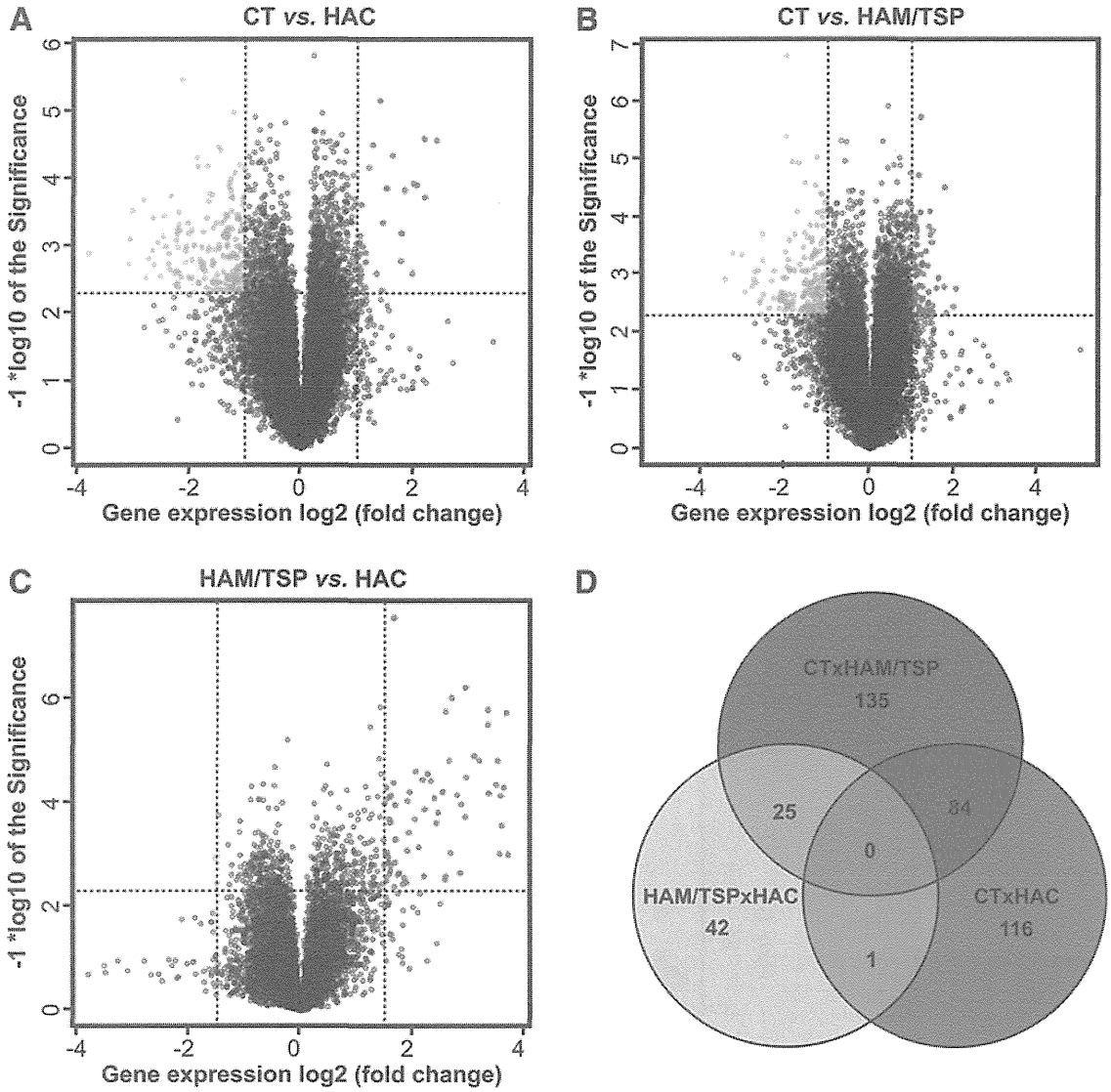

FIG. 2. Differently expressed genes among the CT, HAC, and HAM/TSP groups. Differently expressed genes between the CT and HAC groups **(A)**, CT and HAM/TSP groups **(B)**, and HAC and HAM/TSP groups **(C)** represented by Volcano Plot. Overexpressed genes right are on the upper side and underexpressed genes are on the upper left side. Dots in the middle of the figure represent genes for which the expression showed no statistical difference (Euclidian distance – complete linkage). **(D)** Venn diagram representation of differentially expressed genes. Venn diagrams showed an overlap of genes that are commonly expressed in the three clinical states. CT, healthy control; HAC, asymptomatic HTLV-1 carrier; HAM/TSP, HTLV-1-associated myelopathy/tropical spastic paraparesis.

Spearman's correlation test and verified that the *Gzma*, *Gzmb*, and *Prf1* genes were positively correlated with *Foxp3* gene expression (Fig. 5A–C). We evaluated whether all the genes analyzed in this study (*Pxn*, *Cxcr4*, *IL27*, *Gzma*, *Gzmb*, *Prf1*, and *Foxp3* genes) were correlated with TAX viral protein expression and PVL values. However, only the *Prf1* and *Foxp3* genes presented a positive correlation with TAX expression and the PVL (Fig. 5D–G).

$CD4^+FOXP3^+$ cell percentage was increased in HTLV-1-infected individuals

The phenotype $CD4^+FOXP3^+$ is used to identify a major population of Tregs.[32] Thus we analyzed $CD4^+FOXP3^+$ cell percentage in the CT, HAC, and HAM/TSP groups. The percentage of $CD4^+FOXP3^+$ cells was consistently higher ($p=0.0017$) in HTLV-1-infected individuals than in the CT group (Fig. 5H). The analyses have revealed an increase ($8\times$) in the HAC group compared to the CT group ($p=0.0016$) and an increase ($3\times$) in the HAM/TSP group compared to the CT group ($p=0.0128$) (data not shown).

Discussion

We demonstrated that the gene expression profile in $CD4^+$ T cells differs between the HAC and HAM/TSP groups regardless of TAX expression. It has been well established that HAM/TSP individuals have an HTLV-1 PVL and TAX expression higher than asymptomatic individuals.[33–36] These findings suggest that the risk of HTLV-1 inflammatory diseases strongly correlates with PVL.[37] Here, we demonstrated that PVL and TAX expression of $CD4^+$ T cells positively

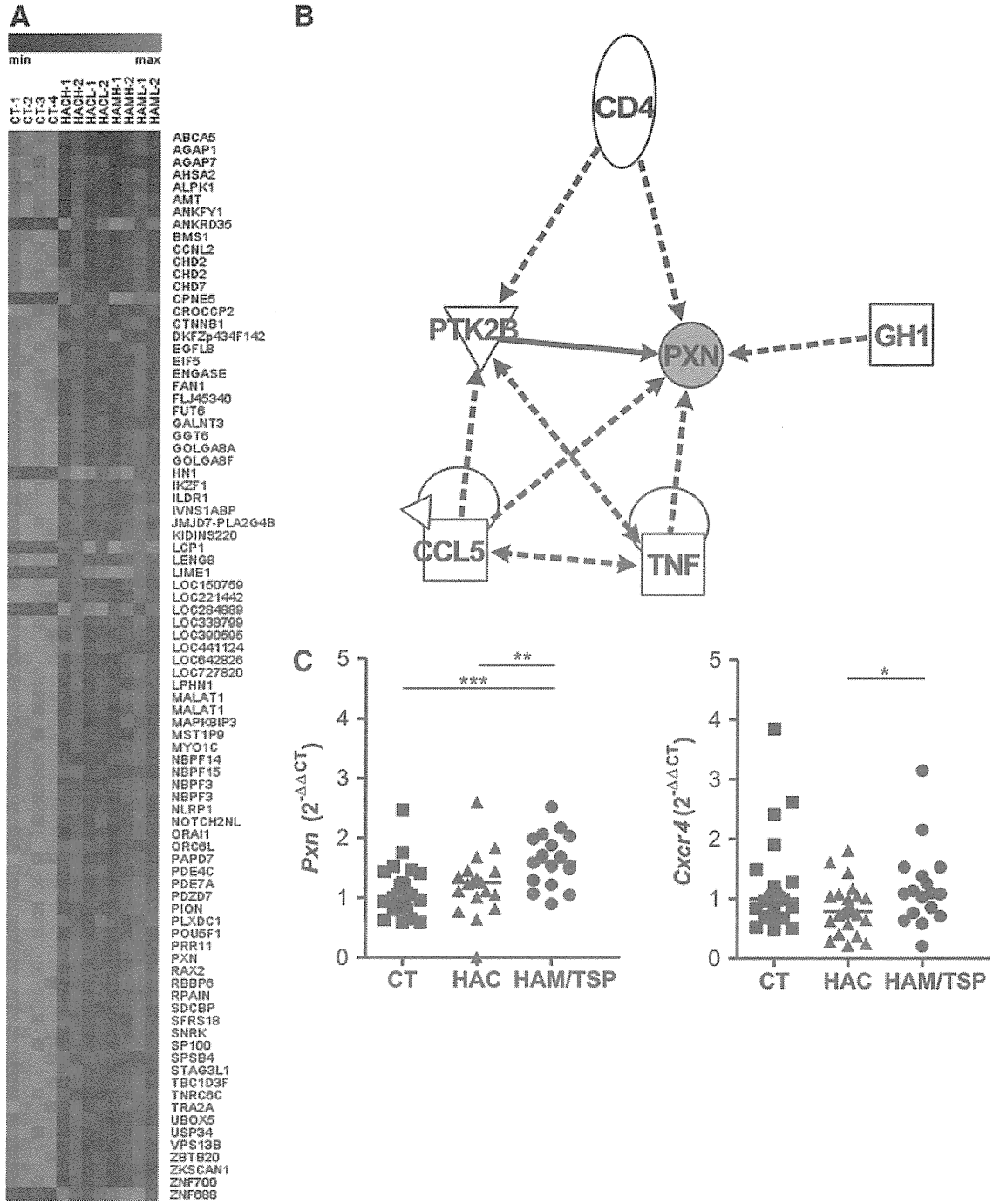

FIG. 3. Expression profiling of genes differentially expressed in HTLV-1. **(A)** Gene expression heat map of analyses of 84 differently expressed genes between the CT vs. HAC and the CT vs. HAM/TSP groups. **(B)** Schematic of molecular interactions. The network image was created using IPA software. The lines represent regulation of function between two genes. **(C)** Real-time PCR of *Pxn* and *Cxcr4* mRNA in $CD4^+$ T cells from CT, HAC, and HAM/TSP. The Mann–Whitney *U*-test was used to evaluate differences among groups (*$p \leq 0.05$; ** $p \leq 0.01$; ***$p \leq 0.001$). CT, healthy control; HAC, asymptomatic HTLV-1 carrier; HAM/TSP, HTLV-1-associated myelopathy/tropical spastic paraparesis.

correlated in HTLV-1-infected groups, being higher in the HAM/TSP group. This observation reinforced the fact that these cells may contribute to the progression of HTLV-1-related diseases.[25,33] Although several authors have published TAX expression and PVL quantification values in HTLV-1-infected individuals, the standard reference values for these parameters have not been well established yet. In our study, we measured the levels of TAX expression and by setting the median value we defined low and high TAX expression samples. Hierarchical clustering analysis showed that CT and HTLV-1-infected groups clustered separately. Here, we also show that $CD4^+$ T cells from HAC and HAM/TSP samples clustered separately regardless of TAX expression. Thus, our results demonstrate that genes are differentially expressed according to individuals' HTLV clinical status in $CD4^+$ T cells. However, it would be important to analyze

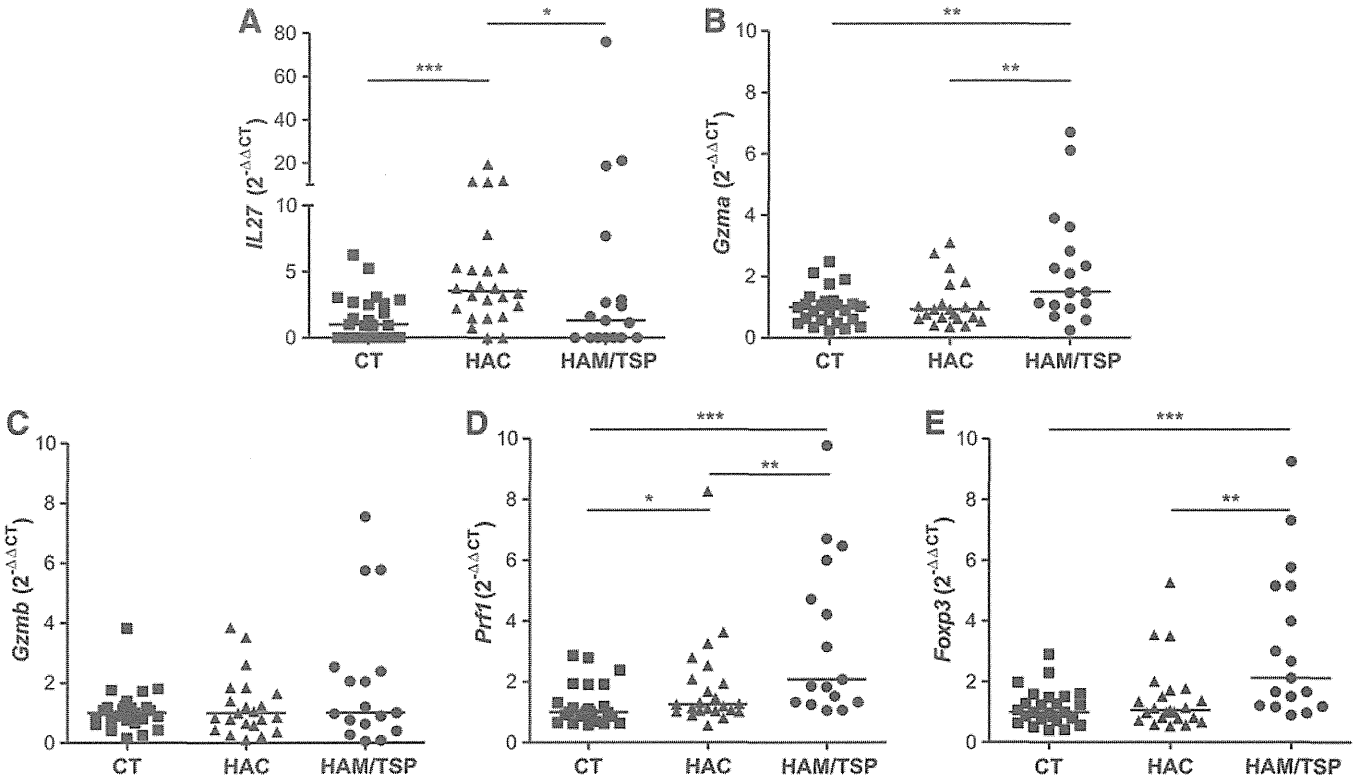

FIG. 4. *IL27*, *Gzma*, *Gzmb*, *Prf1*, and *Foxp3* gene expression by real-time PCR. Gene expression levels comparison of *IL27* **(A)**, *Gzma* **(B)**, *Gzmb* **(C)**, *Prf1* **(D)**, and *Foxp3* **(E)** among the CT, HAC, and HAM/TSP groups. The Mann–Whitney *U*-test was used to evaluate differences among groups (*$p \leq 0.05$; **$p \leq 0.01$; ***$p \leq 0.001$). CT, healthy control; HAC, asymptomatic HTLV-1 carrier; HAM/TSP, HTLV-1-associated myelopathy/tropical spastic paraparesis.

gene expression between the HAC and HAM/TSP groups with similar levels of TAX expression and PVL.

It was reported that the global gene expression profile did not allow observation of two independent clusters for HAC and HAM/TSP; however, ATLL samples were suitably clustered independently.[38] Another previous study did not find differences between the HAC and HAM/TSP groups when clustering $CD4^+$ T cells.[37] These findings could be explained by how the sampling was done. In our analysis, individual samples were submitted to microarray analysis.

We analyzed *Pxn* and *Cxcr4* gene expression since they are involved in cell migration. In response to its binding ligand stromal cell-derived factor-1 (SDF-1), CXCR4 induces downstream signaling by several different pathways. SDF-1 binding to CXCR4 promotes actin polymerization to initiate cell motility. CXCR4 triggers the activation of the src family of protein tyrosine kinases and then the focal adhesion complexes such as RAFTK/Pyk2, focal adhesion kinase, Crk, and paxillin are phosphorylated and activated.[39–41] The focal adhesion components paxillin and Crk play a critical role in the chemotactic signaling pathways.[42]

Although the *Cxcr4* gene did not show deregulation in microarray analysis, the *Pxn* gene is a member of the *Cxcr4* pathway. The *Pxn* gene was overexpressed in the CT group compared to the HTLV-1-infected group in microarray analysis. Intriguingly, after a validation process this gene was significantly up-regulated in the HTLV-1-infected group (HAC+ HAM/TSP). The discordant results between microarray and qPCR techniques are explained by the inherent pitfalls of each technique.[43–47] To confirm the gene expression results obtained from microarray analysis qPCR is frequently used as a validation tool. Furthermore, many different platforms exist for both microarray and qPCR analyses that have led to debates over which techniques produce the most exact measurements of gene expression.[48–50] Additionally, we can also explain our discrepant results based on the fact that microarray and qPCR were not performed with the same number of samples.

CXCR4 is highly expressed by leukocytes in the immune and central nervous systems.[51,52] In this study, *Cxcr4* gene expression was up-regulated in the HAM/TSP group compared to the HAC group and no difference in CXCR4 protein levels by flow cytometry was observed among the studied groups. These different results between *Cxcr4* mRNA and protein expression can be explained by the fact that there are posttranscriptional mechanisms that might control the translation of the protein. The presence of this posttranscriptional control is demonstrated in many studies, suggesting that there is a poor correlation between the mRNA and protein pools in eukaryotic cells.[53–58]

On the other hand, one previous study demonstrated that CXCR4 levels in HTLV-1-infected cell lines were lower than in noninfected cell lines.[59] This could be explained by the type of cell samples used, since we are working with cells belonging to HTLV-1-infected individuals, in which genetic susceptibility should be taken into account. It was also demonstrated that the inhibition of the SDF-1α-CXCR4 axis by the CXCR4 antagonist AMD3100 suppresses the migration of cultured cells from ATL patients and murine lymphoblastoid cells from HTLV-1 TAX transgenic mice. Therefore, these results show the association of the SDF-1alpha/CXCR4 interaction as

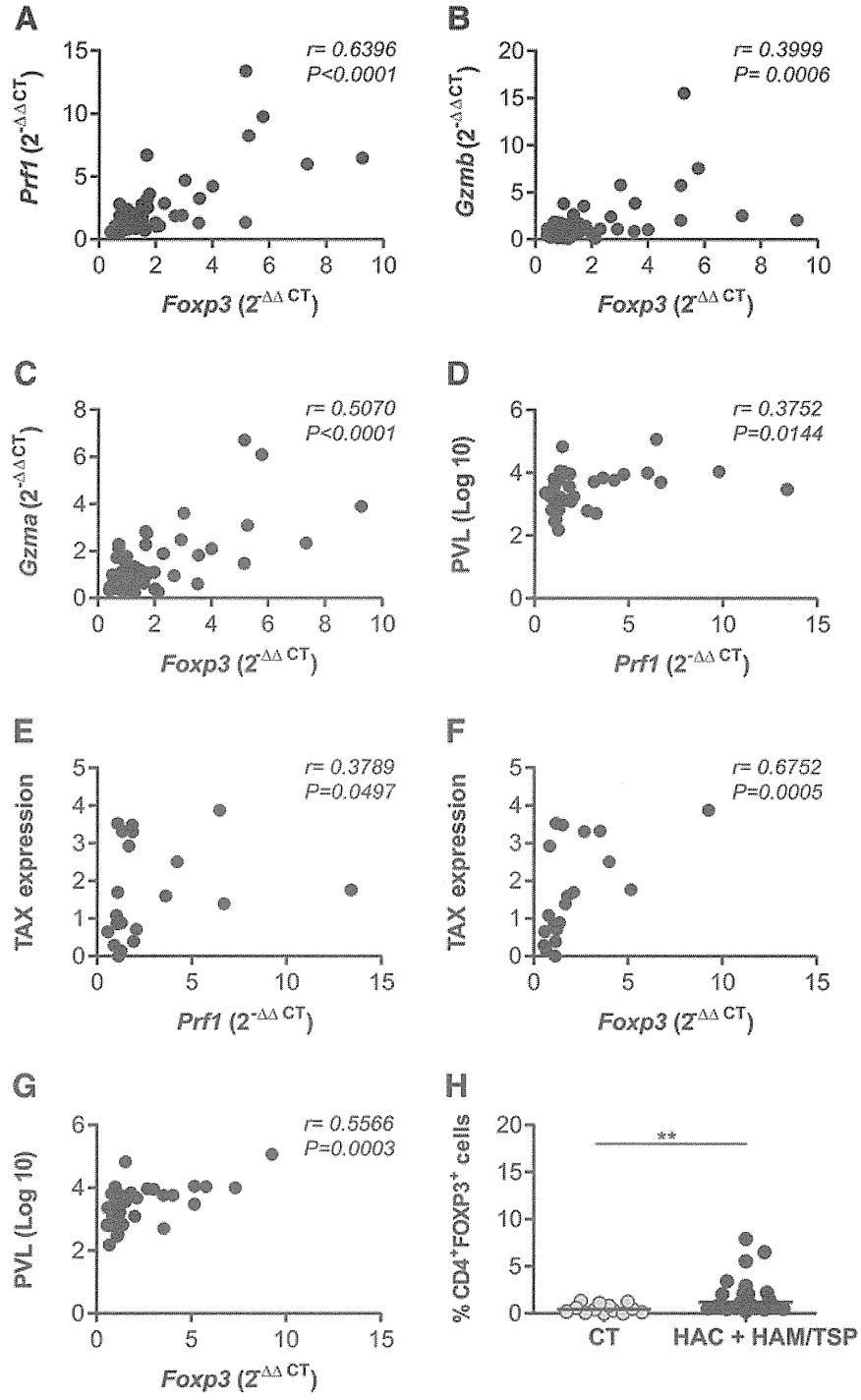

FIG. 5. Correlation between cell lysis-related genes and *Foxp3* in $CD4^+$ T cells, percentage of TAX expression, and proviral load in peripheral blood mononuclear cells (PBMCs). The *Foxp3* expression in $CD4^+$ T cells positively correlated with *Prf1* **(A)**, *Gzmb* **(B)**, and *Gzma* **(C)** expression. A positive correlation between PVL and *Prf1* **(D)**, TAX expression and *Prf1* **(E)**, TAX expression and *Foxp3* **(F)**, and PVL and *Foxp3* **(G)** was observed. The correlation was calculated by the Spearman method. **(H)** The percentage of FOXP3-expressing cells in the $CD4^+$ population from PBMCs. The Mann–Whitney *U*-test was used to evaluate differences among groups ($^{**}p \leq 0.01$). CT, healthy control; HAC, asymptomatic HTLV-1 carrier; HAM/TSP, HTLV-1-associated myelopathy/tropical spastic paraparesis; PVL, proviral load.

one mechanism of leukemic cell migration and this may offer a new target as part of combination therapy for ATLL.[60]

HTLV-1-infected lymphocytes may cross the blood–brain barrier and may generate an intensive immune response leading to the development of HAM/TSP. All the aforementioned findings lead us to believe that there is a dynamic regulation of *Cxcr4* expression, since the *Pxn* and *Cxcr4* genes are overexpressed in the HAM/TSP group. This result suggests that this pathway could be deregulated in these patients and could lead to $CD4^+$ T cell migration to the CNS. This way, our data suggest that the *Pxn* and *Cxcr4* genes may be acting together in $CD4^+$ T cells.

We observed that the *IL27* gene was up-regulated in the HAC group when compared to the CT and HAM/TSP groups. IL-27 is a member of the IL-12 cytokine family and has many functions in immune response such as induction of proliferation of naive specificity and also as an early product of activated antigen-presenting cells.[61] Moreover, it has been shown that IL-27 is capable of regulating T helper subpopulations (Th1, Th2, and Th17) during acute and chronic infection and inflammatory processes.[62–66] Previous studies have reported that IL-27 inhibits HIV-1 replication in T cells and macrophages and HCV replication.[67–70] Furthermore, IL-27 may play an antiviral and antitumor role in ATLL and other

lymphoid malignancies[71] and it has gathered considerable attention in terms of its therapeutic application in immune disease. This way, IL-27 was shown to suppress experimental autoimmune encephalomyelitis during bone marrow stromal cell treatment.[72] Other studies reported suppression of experimental autoimmune uveoretinitis (EAU),[73] inflammation in the joint, and severe arthritis by administration of IL-27. In addition, IL-27 administered *in vivo* showed its anti-inflammatory effects on a delayed type hypersensitivity model, demonstrating its therapeutic potential against some diseases of immune origin.[74] However, IL-27 may be an effective therapeutic agent for HTLV-1-infected individuals in order to suppress the inflammation caused by retroviruses and consequently to decrease the risk of HAM/TSP development. Therefore, the specific role of this cytokine in HTLV-1 infection remains unclear.

The perforin/granzyme mechanism is mainly carried out by circulating white blood cells such as CTLs and natural killer (NK) cells. Several studies have shown that Treg cells may use the perforin/granzyme pathway as a system to suppress the function of immune cells by killing them.[31,75,76] It was demonstrated that activated murine Treg cells suppressed B cell proliferation in a granzyme B- and perforin-dependent fashion.[76] Likewise, the activated human Treg cells expressed granzyme A and/or B and could use the perforin pathway to cause autologous target cell death.[75] The transcriptional factor FOXP3 is considered one of the main specific markers for Treg cells[77] whose expression is a critical mediator for the development and the function of these cells.[78] Treg cells are major effector cells during immune response by the perforin/granzyme pathway. Considering this, we selected *Gzma*, *Gzmb*, *Prf1*, and *Foxp3* for gene expression analysis.

The level of *Prf1* and *Gzma* gene expression was significantly higher in the HAM/TSP group compared to the CT and HAC groups. No differences were observed in intracellular PRF1 among the studied groups. Protein detection and quantification are potent tools since mRNA detection could not guarantee that protein will be translated or functional. Thus there could be posttranscriptional mechanisms that regulate the expression of these molecules. Moreover, measurement of granzyme and perforin mRNA is better than immunostaining of granzyme and perforin proteins as a correlate of cytotoxicity, because the granzyme and perforin proteins do not accumulate in the cell but are rapidly and continually discharged in the lytic granules.[37] Therefore, all these considerations can explain our results.

Although it has been demonstrated that HTLV-1 has a tropism to Treg cells,[79] reduced FOXP3 protein expression in HTLV-1-infected cells of HAM/TSP patients has been reported.[80,81] However, in our analysis of *Foxp3* gene expression, we also noticed a significant increase in the HAM/TSP group compared to the CT and HAC groups. We also observed a positive correlation among *Gzma*, *Gzmb*, and *Prf1* to *Foxp3*. In addition to that, there was also a positive correlation between the *Foxp3* gene and PVL and the *Foxp3* gene and TAX expression. These data are consistent with the results from a previous report[82] describing higher $FOXP3^+$ expression in $CD4^+$ T cells of individuals with HAM/TSP compared to healthy individuals. In addition, the researchers have also observed a positive correlation between FOXP3 and PVL and FOXP3 and TAX expression. We also found an increased frequency of $CD4^+FOXP3^+$ cells in HTLV-1-infected individuals, as reported previously.[82,83] In our results, we showed that *Foxp3* gene expression levels were increased in the HAM/TSP group compared to the HAC group, while the proportions of $CD4^+FOXP3^+$ cells were higher in the HAC group compared to the HAM/TSP group. This discordance may be due to differences between both applied techniques. In general, the sensitivity of real-time RT-PCR is higher than that of flow cytometry.[84]

Many studies on solid-organ transplant recipients (heart, kidney, and intestine) have demonstrated a direct correlation between Treg marker FOXP3 and the cytotoxic T cell effector molecules (granzyme B, perforin, and granulysin) in the process of acute rejection.[85–89] Therefore, in our study we speculate that FOXP3 is correlated with the cytotoxic T cell effector molecules (*Gzma*, *Gzmb*, and *Prf1*) in HTLV-1 infection. One previous study suggested two possibilities for the role of Treg cells in HTLV-1 infection. First, $FOXP3^+$ T cells have hyperproliferation ability[90] and this could collaborate in the clonal expansion of HTLV-1-infected cells. Second, HTLV-1 can invade the immune system by direct infection of this immunosuppressive cell population. Consequently, HTLV-1 infection of $FOXP3^+$ T cells can enable the virus to increase or maintain its proviral load and thus reach a state of persistent infection.[91] With this in mind, we suggest another possibility for the role of Treg cells. Treg cells may use the perforin/granzyme pathway as a system to suppress the immune cells by killing them. This way, the increase of $FOXP3^+$ T cells analyzed in HTLV-1 infection may contribute to immunodeficiency, which is observed in HTLV-1 infection.[92]

In a previous study, we reported differentially expressed genes in $CD8^+$ T cells isolated from the same population as this study. Our results showed that patients with HAM/TSP have high expression levels of degranulation-related genes (*Gzmh* and *Prf1*) and of the cytoskeletal adaptor *Pxn*. We indicated that *Gzmb* and *Zap70* genes were overexpressed in HTLV-infected individuals compared to the healthy control group. We also found that *Ccl5* was higher in the HAM/TSP group compared to the HAC and CT groups. Therefore, our findings showed that $CD8^+$ and $CD4^+$ T cells from HAM/TSP patients have an inflammatory and active profile.[93]

In conclusion, we demonstrated that *Pxn*, *Cxcr4*, *IL27*, and *Gzma* gene expression in $CD4^+$ T cells differs between the HAC and HAM/TSP groups regardless of TAX expression. *Prf1* and *Foxp3* genes are increased in the HAM/TSP group compared to the HAC group and present a positive correlation to the expression of TAX and PVL. We believe that the *IL27*, *Pxn*, *Cxcr4*, *Gzma*, *Prf1*, and *Foxp3* genes are novel molecules that could play an important role in HTLV-1 infection. Moreover, Treg may be a future strategy for the treatment and prevention of HTLV-1-infected individuals. However, further studies are required to elucidate the molecular mechanisms of $CD4^+$ T cell involved in HTLV-1 infection.

Acknowledgments

The authors thank Rochele Azevedo for quantification of the proviral load, Patrícia Vianna Bonini Palma for flow cytometry analysis, Amelia Goes de Araujo for her assistance with the microarray technique, Maurício Cristiano Rocha Junior for help in writing the paper, and Prof. Charles Bangham

for TAX expression analysis. They are also grateful to the patients. This work was supported by Fundação Hemocentro de Ribeirão Preto (FUNDHERP) and São Paulo Research Foundation (FAPESP-Process number: 2011/21740-7)

Author Disclosure Statement

No competing financial interests exist.

References

1. Poiesz BJ, Ruscetti FW, Gazdar AF, *et al.:* Detection and isolation of type C retrovirus particles from fresh and cultured lymphocytes of a patient with cutaneous T-cell lymphoma. Proc Natl Acad Sci USA 1980;77(12):7415–7419.
2. Gessain A, Barin F, Vernant JC, *et al.:* Antibodies to human T-lymphotropic virus type-I in patients with tropical spastic paraparesis. Lancet 1985;2:407–410.
3. Osame M, Usuku K, Izumo S, *et al.:* HTLV-I associated myelopathy, a new clinical entity. Lancet 1986;1(8488):1031–1032.
4. Uchiyama T, Yodoi J, Sagawa K, *et al.:* Adult T-cell leukemia: Clinical and hematologic features of 16 cases. Blood 1977;50(3):481–492.
5. Yoshida M, Seiki M, Yamaguchi K, *et al.:* Monoclonal integration of human T-cell leukemia provirus in all primary tumors of adult T-cell leukemia suggests causative role of human T-cell leukemia virus in the disease. Proc Natl Acad Sci USA 1984;81(8):2534–2537.
6. LaGrenade L, Hanchard B, Fletcher V, *et al.:* Infective dermatitis of Jamaican children: A marker for HTLV-I infection. Lancet 1990;336(8727):1345–1347.
7. Mariette X, Agbalika F, Zucker-Franklin D, *et al.:* Detection of the tax gene of HTLV-I in labial salivary glands from patients with Sjogren's syndrome and other diseases of the oral cavity. Clin Exp Rheumatol 2000;18(3):341–347.
8. Mochizuki M, Ono A, Ikeda E, *et al.:* HTLV-I uveitis. J Acquir Immune Defic Syndr Hum Retrovirol 1996;13(Suppl 1):S50–56.
9. Morgan OS, Rodgers-Johnson P, Mora C, *et al.:* HTLV-1 and polymyositis in Jamaica. Lancet 1989;2(8673):1184–1187.
10. Nishioka K, Maruyama I, Sato K, *et al.:* Chronic inflammatory arthropathy associated with HTLV-I. Lancet 1989; 1(8635):441.
11. Kaplan TA: Low-lying disordered states when ground-state long-range order exists; large-amplitude spin waves. Phys Rev B Condens Matter 1990;41(10):6882–6888.
12. Murphy EL, Figueroa JP, Gibbs WN, *et al.:* Sexual transmission of human T-lymphotropic virus type I (HTLV-I). Ann Intern Med 1989;111(7):555–560.
13. Catalan-Soares B, Carneiro-Proietti AB, and Proietti FA: Heterogeneous geographic distribution of human T-cell lymphotropic viruses I and II (HTLV-I/II): Serological screening prevalence rates in blood donors from large urban areas in Brazil. Cad Saude Publica 2005;21(3):926–931.
14. Dourado I, Alcantara LC, Barreto ML, *et al.:* HTLV-I in the general population of Salvador, Brazil: A city with African ethnic and sociodemographic characteristics. J Acquir Immune Defic Syndr 2003;34(5):527–531.
15. Matsuura E, Yamano Y, and Jacobson S: Neuroimmunity of HTLV-I infection. J Neuroimmune Pharmacol 2010;5(3): 310–325.
16. Araujo AQ and Silva MT: The HTLV-1 neurological complex. Lancet Neurol 2006;5(12):1068–1076.
17. Vernant JC, Maurs L, Gessain A, *et al.:* Endemic tropical spastic paraparesis associated with human T-lymphotropic virus type I: A clinical and seroepidemiological study of 25 cases. Ann Neurol 1987;21(2):123–130.
18. Lima MA, Bica RB, and Araujo AQ: Gender influence on the progression of HTLV-I associated myelopathy/tropical spastic paraparesis. J Neurol Neurosurg Psychiatry 2005; 76(2):294–296.
19. Nakagawa M, Izumo S, Ijichi S, *et al.:* HTLV-I-associated myelopathy: Analysis of 213 patients based on clinical features and laboratory findings. J Neurovirol 1995;1(1):50–61.
20. Chang SC, Cheng JC, Kou YH, *et al.:* Roles of the AX(4)GKS and arginine-rich motifs of hepatitis C virus RNA helicase in ATP- and viral RNA-binding activity. J Virol 2000;74(20): 9732–9737.
21. Taylor JM and Nicot C: HTLV-1 and apoptosis: Role in cellular transformation and recent advances in therapeutic approaches. Apoptosis 2008;13(6):733–747.
22. Richardson JH, Edwards AJ, Cruickshank JK, *et al.:* In vivo cellular tropism of human T-cell leukemia virus type 1. J Virol 1990;64(11):5682–5687.
23. Umehara F, Izumo S, Nakagawa M, *et al.:* Immunocytochemical analysis of the cellular infiltrate in the spinal cord lesions in HTLV-I-associated myelopathy. J Neuropathol Exp Neurol 1993;52(4):424–430.
24. Umehara F, Izumo S, Ronquillo AT, *et al.:* Cytokine expression in the spinal cord lesions in HTLV-I-associated myelopathy. J Neuropathol Exp Neurol 1994;53(1):72–77.
25. Goon PK, Igakura T, Hanon E, *et al.:* Human T cell lymphotropic virus type I (HTLV-I)-specific CD4+ T cells: Immunodominance hierarchy and preferential infection with HTLV-I. J Immunol 2004;172(3):1735–1743.
26. Nose H, Kubota R, Seth NP, *et al.:* Ex vivo analysis of human T lymphotropic virus type 1-specific CD4+ cells by use of a major histocompatibility complex class II tetramer composed of a neurological disease-susceptibility allele and its immunodominant peptide. J Infect Dis 2007;196(12): 1761–1772.
27. De Castro-Costa CM, Araujo AQ, Barreto MM, *et al.:* Proposal for diagnostic criteria of tropical spastic paraparesis/ HTLV-I-associated myelopathy (TSP/HAM). AIDS Res Hum Retroviruses 2006;22(10):931–935.
28. Pinto MT, Rodrigues ES, Malta TM, *et al.:* HTlV-1/2 Seroprevalence and coinfection rate in Brazilian first-time blood donors: An 11-year follow-up. Rev Inst Med Trop Sao Paulo 2012;54(3):123–129.
29. Vandesompele J, De Preter K, Pattyn F, *et al.:* Accurate normalization of real-time quantitative RT-PCR data by geometric averaging of multiple internal control genes. Genome Biol 2002;3(7):RESEARCH0034.
30. Pfaffl MW: A new mathematical model for relative quantification in real-time RT-PCR. Nucleic Acids Res 2001; 29(9):e45.
31. Cao X, Cai SF, Fehniger TA, *et al.:* Granzyme B and perforin are important for regulatory T cell-mediated suppression of tumor clearance. Immunity 2007;27(4):635–646.
32. Ziegler SF: FOXP3: Of mice and men. Annu Rev Immunol 2006;24:209–226.
33. Goon PK, Hanon E, Igakura T, *et al.:* High frequencies of Th1-type CD4(+) T cells specific to HTLV-1 Env and Tax proteins in patients with HTLV-1-associated myelopathy/ tropical spastic paraparesis. Blood 2002;99(9):3335–3341.
34. Hashimoto K, Higuchi I, Osame M, *et al.:* Quantitative in situ PCR assay of HTLV-1 infected cells in peripheral blood

lymphocytes of patients with ATL, HAM/TSP and asymptomatic carriers. J Neurol Sci 1998;159(1):67–72.
35. Kubota R, Kawanishi T, Matsubara H, *et al.:* Demonstration of human T lymphotropic virus type I (HTLV-I) tax-specific CD8+ lymphocytes directly in peripheral blood of HTLV-I-associated myelopathy/tropical spastic paraparesis patients by intracellular cytokine detection. J Immunol 1998;161(1): 482–488.
36. Nagai M, Usuku K, Matsumoto W, *et al.:* Analysis of HTLV-I proviral load in 202 HAM/TSP patients and 243 asymptomatic HTLV-I carriers: High proviral load strongly predisposes to HAM/TSP. J Neurovirol 1998; 4(6):586–593.
37. Vine AM, Heaps AG, Kaftantzi L, *et al.:* The role of CTLs in persistent viral infection: Cytolytic gene expression in CD8+ lymphocytes distinguishes between individuals with a high or low proviral load of human T cell lymphotropic virus type 1. J Immunol 2004;173(8):5121–5129.
38. Oliere S, Hernandez E, Lezin A, *et al.:* HTLV-1 evades type I interferon antiviral signaling by inducing the suppressor of cytokine signaling 1 (SOCS1). PLoS Pathog 2010;6(11): e1001177.
39. Fernandis AZ, Prasad A, Band H, *et al.:* Regulation of CXCR4-mediated chemotaxis and chemoinvasion of breast cancer cells. Oncogene 2004;23(1):157–167.
40. Hartmann TN, Burger JA, Glodek A, *et al.:* CXCR4 chemokine receptor and integrin signaling co-operate in mediating adhesion and chemoresistance in small cell lung cancer (SCLC) cells. Oncogene 2005;24(27):4462–4471.
41. Luker KE and Luker GD: Functions of CXCL12 and CXCR4 in breast cancer. Cancer Lett 2006;238(1):30–41.
42. Ganju RK, Brubaker SA, Meyer J, *et al.:* The alpha-chemokine, stromal cell-derived factor-1alpha, binds to the transmembrane G-protein-coupled CXCR-4 receptor and activates multiple signal transduction pathways. J Biol Chem 1998; 273(36):23169–23175.
43. Bustin SA: Quantification of mRNA using real-time reverse transcription PCR (RT-PCR): Trends and problems. J Mol Endocrinol 2002;29(1):23–39.
44. Chuaqui RF, Bonner RF, Best CJ, *et al.:* Post-analysis follow-up and validation of microarray experiments. Nat Genet 2002;32(Suppl):509–514.
45. Freeman WM, Walker SJ, and Vrana KE: Quantitative RT-PCR: Pitfalls and potential. Biotechniques 1999;26(1): 112–122, 124–125.
46. Wurmbach E, Yuen T, and Sealfon SC: Focused microarray analysis. Methods 2003;31(4):306–316.
47. Yang YH, Dudoit S, Luu P, *et al.:* Normalization for cDNA microarray data: A robust composite method addressing single and multiple slide systematic variation. Nucleic Acids Res 2002;30(4):e15.
48. Tan PK, Downey TJ, Spitznagel EL Jr, *et al.:* Evaluation of gene expression measurements from commercial microarray platforms. Nucleic Acids Res 2003;31(19):5676–5684.
49. Yauk CL, Berndt ML, Williams A, *et al.:* Comprehensive comparison of six microarray technologies. Nucleic Acids Res 2004;32(15):e124.
50. Zhu B, Ping G, Shinohara Y, *et al.:* Comparison of gene expression measurements from cDNA and 60-mer oligonucleotide microarrays. Genomics 2005;85(6):657–665.
51. Jazin EE, Soderstrom S, Ebendal T, *et al.:* Embryonic expression of the mRNA for the rat homologue of the fusin/CXCR-4 HIV-1 co-receptor. J Neuroimmunol 1997;79(2): 148–154.
52. Moepps B, Frodl R, Rodewald HR, *et al.:* Two murine homologues of the human chemokine receptor CXCR4 mediating stromal cell-derived factor 1alpha activation of Gi2 are differentially expressed in vivo. Eur J Immunol 1997; 27(8):2102–2112.
53. Ideker T, Thorsson V, Ranish JA, *et al.:* Integrated genomic and proteomic analyses of a systematically perturbed metabolic network. Science 2001;292(5518):929–934.
54. Greenbaum D, Colangelo C, Williams K, *et al.:* Comparing protein abundance and mRNA expression levels on a genomic scale. Genome Biol 2003;4(9):117.
55. Gygi SP, Rochon Y, Franza BR, *et al.:* Correlation between protein and mRNA abundance in yeast. Mol Cell Biol 1999;19(3):1720–1730.
56. Schwanhausser B, Busse D, Li N, *et al.:* Global quantification of mammalian gene expression control. Nature 2011; 473(7347):337–342.
57. Ghazalpour A, Bennett B, Petyuk VA, *et al.:* Comparative analysis of proteome and transcriptome variation in mouse. PLoS Genet 2011;7(6):e1001393.
58. Vogel C and Marcotte EM: Insights into the regulation of protein abundance from proteomic and transcriptomic analyses. Nat Rev Genet 2012;13(4):227–232.
59. Arai M, Ohashi T, Tsukahara T, *et al.:* Human T-cell leukemia virus type 1 Tax protein induces the expression of lymphocyte chemoattractant SDF-1/PBSF. Virology 1998; 241(2):298–303.
60. Kawaguchi A, Orba Y, Kimura T, *et al.:* Inhibition of the SDF-1alpha-CXCR4 axis by the CXCR4 antagonist AMD3100 suppresses the migration of cultured cells from ATL patients and murine lymphoblastoid cells from HTLV-I Tax transgenic mice. Blood 2009;114(14):2961–2968.
61. Pflanz S, Timans JC, Cheung J, *et al.:* IL-27, a heterodimeric cytokine composed of EBI3 and p28 protein, induces proliferation of naive CD4(+) T cells. Immunity 2002;16(6): 779–790.
62. Niedbala W, Cai B, Wei X, *et al.:* Interleukin 27 attenuates collagen-induced arthritis. Ann Rheum Dis 2008;67(10): 1474–1479.
63. Batten M, Li J, Yi S, *et al.:* Interleukin 27 limits autoimmune encephalomyelitis by suppressing the development of interleukin 17-producing T cells. Nat Immunol 2006;7(9): 929–936.
64. Hamano S, Himeno K, Miyazaki Y, *et al.:* WSX-1 is required for resistance to Trypanosoma cruzi infection by regulation of proinflammatory cytokine production. Immunity 2003; 19(5):657–667.
65. Stumhofer JS, Laurence A, Wilson EH, *et al.:* Interleukin 27 negatively regulates the development of interleukin 17-producing T helper cells during chronic inflammation of the central nervous system. Nat Immunol 2006;7(9):937–945.
66. Yoshimura T, Takeda A, Hamano S, *et al.:* Two-sided roles of IL-27: Induction of Th1 differentiation on naive CD4+ T cells versus suppression of proinflammatory cytokine production including IL-23-induced IL-17 on activated CD4+ T cells partially through STAT3-dependent mechanism. J Immunol 2006;177(8):5377–5385.
67. Fakruddin JM, Lempicki RA, Gorelick RJ, *et al.:* Noninfectious papilloma virus-like particles inhibit HIV-1 replication: Implications for immune control of HIV-1 infection by IL-27. Blood 2007;109(5):1841–1849.
68. Frank AC, Zhang X, Katsounas A, *et al.:* Interleukin-27, an anti-HIV-1 cytokine, inhibits replication of hepatitis C virus. J Interferon Cytokine Res 2010;30(6):427–431.

69. Greenwell-Wild T, Vazquez N, Jin W, *et al.:* Interleukin-27 inhibition of HIV-1 involves an intermediate induction of type I interferon. Blood 2009;114(9):1864–1874.
70. Imamichi T, Yang J, Huang DW, *et al.:* IL-27, a novel anti-HIV cytokine, activates multiple interferon-inducible genes in macrophages. AIDS 2008;22(1):39–45.
71. Larousserie F, Bardel E, Pflanz S, *et al.:* Analysis of interleukin-27 (EBI3/p28) expression in Epstein-Barr virus- and human T-cell leukemia virus type 1-associated lymphomas: Heterogeneous expression of EBI3 subunit by tumoral cells. Am J Pathol 2005;166(4):1217–1228.
72. Wang J, Wang G, Sun B, *et al.:* Interleukin-27 suppresses experimental autoimmune encephalomyelitis during bone marrow stromal cell treatment. J Autoimmun 2008;30(4):222–229.
73. Amadi-Obi A, Yu CR, Liu X, *et al.:* TH17 cells contribute to uveitis and scleritis and are expanded by IL-2 and inhibited by IL-27/STAT1. Nat Med 2007;13(6):711–718.
74. Miyazaki Y, Shimanoe Y, Wang S, *et al.:* Amelioration of delayed-type hypersensitivity responses by IL-27 administration. Biochem Biophys Res Commun 2008;373(3):397–402.
75. Grossman WJ, Verbsky JW, Barchet W, *et al.:* Human T regulatory cells can use the perforin pathway to cause autologous target cell death. Immunity 2004;21(4):589–601.
76. Zhao DM, Thornton AM, DiPaolo RJ, *et al.:* Activated CD4+CD25+ T cells selectively kill B lymphocytes. Blood 2006;107(10):3925–3932.
77. Hori S, Nomura T, and Sakaguchi S: Control of regulatory T cell development by the transcription factor Foxp3. Science 2003;299(5609):1057–1061.
78. Fontenot JD and Rudensky AY: A well adapted regulatory contrivance: Regulatory T cell development and the forkhead family transcription factor Foxp3. Nat Immunol 2005; 6(4):331–337.
79. Roncador G, Garcia JF, Maestre L, *et al.:* FOXP3, a selective marker for a subset of adult T-cell leukaemia/lymphoma. Leukemia 2005;19(12):2247–2253.
80. Oh U, Grant C, Griffith C, Fugo K, *et al.:* Reduced Foxp3 protein expression is associated with inflammatory disease during human T lymphotropic virus type 1 infection. J Infect Dis 2006;193(11):1557–1566.
81. Hayashi D, Kubota R, Takenouchi N, *et al.:* Reduced Foxp3 expression with increased cytomegalovirus-specific CTL in HTLV-I-associated myelopathy. J Neuroimmunol 2008; 200(1–2):115–124.
82. Toulza F, Heaps A, Tanaka Y, *et al.:* High frequency of CD4+FoxP3+ cells in HTLV-1 infection: Inverse correlation with HTLV-1-specific CTL response. Blood 2008;111(10): 5047–5053.
83. Best I, Lopez G, Verdonck K, *et al.:* IFN-gamma production in response to Tax 161-233, and frequency of CD4+ Foxp3+ and Lin HLA-DRhigh CD123+ cells, discriminate HAM/TSP patients from asymptomatic HTLV-1-carriers in a Peruvian population. Immunology 2009;128(1 Suppl): e777–786.
84. Malec M, van der Velden VH, Bjorklund E, *et al.:* Analysis of minimal residual disease in childhood acute lymphoblastic leukemia: Comparison between RQ-PCR analysis of Ig/TcR gene rearrangements and multicolor flow cytometric immunophenotyping. Leukemia 2004;18(10):1630–1636.
85. Corti B, Altimari A, Gabusi E, *et al.:* Potential of real-time PCR assessment of granzyme B and perforin up-regulation for rejection monitoring in intestinal transplant recipients. Transplant Proc 2005;37(10):4467–4471.
86. Sarwal MM, Jani A, Chang S, *et al.:* Granulysin expression is a marker for acute rejection and steroid resistance in human renal transplantation. Hum Immunol 2001;62(1):21–31.
87. Shin GT, Kim SJ, Lee TS, *et al.:* Gene expression of perforin by peripheral blood lymphocytes as a marker of acute rejection. Nephron Clin Pract 2005;100(3):c63–70.
88. Vlad G, Ho EK, Vasilescu ER, *et al.:* Anti-CD25 treatment and FOXP3-positive regulatory T cells in heart transplantation. Transpl Immunol 2007;18(1):13–21.
89. Shi R, Yang J, Jaramillo A, *et al.:* Correlation between interleukin-15 and granzyme B expression and acute lung allograft rejection. Transpl Immunol 2004;12(2):103–108.
90. Vukmanovic-Stejic M, Zhang Y, Cook JE, *et al.:* Human CD4+ CD25hi Foxp3+ regulatory T cells are derived by rapid turnover of memory populations in vivo. J Clin Invest 2006;116(9):2423–2433.
91. Satou Y, Utsunomiya A, Tanabe J, *et al.:* HTLV-1 modulates the frequency and phenotype of FoxP3+CD4+ T cells in virus-infected individuals. Retrovirology 2012;9:46.
92. Tachibana N, Okayama A, Ishizaki J, *et al.:* Suppression of tuberculin skin reaction in healthy HTLV-I carriers from Japan. Int J Cancer 1988;42(6):829–831.
93. Malta TM, Silva IT, Pinheiro DG, *et al.:* Altered expression of degranulation-related genes in CD8(+) T cells in human T lymphotropic virus Type I infection. AIDS Res Hum Retroviruses 2013;28:826–836.

Address correspondence to:
Simone Kashima
Regional Blood Center of Ribeirão Preto
Rua Tenente Catão Roxo, 2501
14051-140 Ribeirão Preto
São Paulo
Brazil

E-mail: skashima@hemocentro.fmrp.usp.br

OPEN

Citation: Blood Cancer Journal (2013) 3, e132; doi:10.1038/bcj.2013.30

www.nature.com/bcj

ORIGINAL ARTICLE

Oral administration of an HSP90 inhibitor, 17-DMAG, intervenes tumor-cell infiltration into multiple organs and improves survival period for ATL model mice

E Ikebe[1], A Kawaguchi[2,3,13], K Tezuka[4,13], S Taguchi[1,13], S Hirose[1], T Matsumoto[1], T Mitsui[1], K Senba[1], A Nishizono[1], M Hori[5], H Hasegawa[6], Y Yamada[6], T Ueno[4], Y Tanaka[7], H Sawa[3], W Hall[8], Y Minami[9], KT Jeang[10], M Ogata[11], K Morishita[12], H Hasegawa[2], J Fujisawa[4] and H Iha[1]

In the peripheral blood leukocytes (PBLs) from the carriers of the human T-lymphotropic virus type-1 (HTLV-1) or the patients with adult T-cell leukemia (ATL), nuclear factor kappaB (NF-κB)-mediated antiapoptotic signals are constitutively activated primarily by the HTLV-1-encoded oncoprotein Tax. Tax interacts with the I κB kinase regulatory subunit NEMO (NF-κB essential modulator) to activate NF-κB, and this interaction is maintained in part by a molecular chaperone, heat-shock protein 90 (HSP90), and its co-chaperone cell division cycle 37 (CDC37). The antibiotic geldanamycin (GA) inhibits HSP90's ATP binding for its proper interaction with client proteins. Administration of a novel water-soluble and less toxic GA derivative, 17-dimethylaminoethylamino-17-demethoxygeldanamycin hydrochloride (17-DMAG), to Tax-expressing ATL-transformed cell lines, C8166 and MT4, induced significant degradation of Tax. 17-DMAG also facilitated growth arrest and cellular apoptosis to C8166 and MT4 and other ATL cell lines, although this treatment has no apparent effects on normal PBLs. 17-DMAG also downregulated Tax-mediated intracellular signals including the activation of NF-κB, activator protein 1 or HTLV-1 long terminal repeat in Tax-transfected HEK293 cells. Oral administration of 17-DMAG to ATL model mice xenografted with lymphomatous transgenic Lck-Tax (Lck proximal promoter-driven Tax transgene) cells or HTLV-1-producing tumor cells dramatically attenuated aggressive infiltration into multiple organs, inhibited *de novo* viral production and improved survival period. These observations identified 17-DMAG as a promising candidate for the prevention of ATL progression.

Blood Cancer Journal (2013) **3,** e132; doi:10.1038/bcj.2013.30; published online 16 August 2013

Keywords: 17-DMAG; molecular chaperon; Tax; ATL; apoptosis; transgenic model

INTRODUCTION

Nuclear factor kappaB (NF-κB) is a transcription factor that regulates immune and antiapoptotic responses to multiple extracellular stresses.[1,2] Under normal conditions, most NF-κB molecules are sequestered in the cytoplasm by the inhibitor I κB. In response to cellular stress, I κB is rapidly phosphorylated by the NF-κB activator I κB kinase (IKK) and ubiquitylated for degradation by the proteasome. This frees NF-κB for translocation into the nucleus, where it directs the transcriptional activation of NF-κB-responsive genes.[3,4] IKK is comprised of three different subunits, IKKα, IKKβ and IKKγ/NEMO (NF-κB essential modulator). IKKγ is also known as NF-κB essential modulator (NEMO). NEMO trimerizes rapidly in response to extracellular stimuli, such as the pro-inflammatory cytokine tumor necrosis factor-α (TNF-α), and recruits the two catalytic subunits, IKKα/β, to form a highly phosphorylated active IKK holoenzyme.[5] Several genetic studies have shown that cytokine-triggered activation of what is termed the canonical NF-κB activation pathway is primarily dependent on NEMO and IKKβ,[6,7] whereas IKKα activity is required for the development of the skin, limbs and lymph nodes.[8,9] Upon stimulation, several accessory proteins are recruited to IKK, and the molecular size of this active IKK complex reaches more than 1 MDa.[10,11] The molecular chaperone heat-shock protein 90 (HSP90) and its co-chaperone cell division cycle 37 (CDC37) are components of this high molecular weight (HMW)-IKK complex, and they play crucial roles in maintaining the activity of the complex.[12] The antibiotic geldanamycin (GA) specifically binds to the ATPase domain of HSP90 and inhibits its function as a molecular chaperone, resulting in the efficient inhibition of TNF-α-mediated activation of NF-κB.[12,13]

The human T-lymphotropic virus type-1 (HTLV-1), which is the etiologic agent of adult T-cell leukemia (ATL), encodes the oncoprotein Tax.[14–16] Tax activates NF-κB by interacting

[1]Department of Infectious Diseases, Faculty of Medicine, Oita University, Yufu, Japan; [2]Department of Pathology, National Institute of Infectious Diseases, Musashimurayama, Japan; [3]Department of Molecular Pathobiology, 21st Century COE Program for Zoonosis Control, Hokkaido University Research Center for Zoonosis Control, Sapporo, Japan; [4]Department of Microbiology, Kansai Medical University, Moriguchi, Japan; [5]Department of Hematology, Ibaraki Prefectural Central Hospital, Kasama, Ibaraki, Japan; [6]Department of Laboratory Medicine, Nagasaki University Graduate School of Biomedical Sciences, Nagasaki, Japan; [7]Department of Immunology, Graduate School of Medicine, University of the Ryukyus, Nishihara, Japan; [8]Department of Medical Microbiology, Centre for Research in Infectious Diseases, Conway Institute of Biomolecular and Biomedical Research, University College Dublin, Dublin, Ireland; [9]Department of Biotechnology, Maebashi Institute of Technology, Maebashi, Japan; [10]Molecular Virology Section, Laboratory of Molecular Microbiology, National Institute of Allergy and Infectious Diseases, Bethesda, MD, USA; [11]Department of Hematology, Faculty of Medicine, Oita University, Yufu, Japan and [12]Division of Tumor and Cellular Biochemistry, Department of Medical Sciences, Faculty of Medicine, University of Miyazaki, Miyazaki, Japan. Correspondence: Dr H Iha, Department of Infectious Diseases, Faculty of Medicine, Oita University, 1-1 Idaigaoka, Hasama, Yufu, Oita 879-5593, Japan.
E-mail: hiha@oita-u.ac.jp
[13]These authors contributed equally to this work.
Received 25 June 2012; revised 24 June 2013; accepted 28 June 2013

physically with NEMO.[10,17] NF-κB activation mediated by this Tax–NEMO interaction is similar to that of the TNF-α-triggered 'canonical' pathway. Tax induces IKK phosphorylation, ubiquitylation and proteasome-dependent degradation of I κB, thereby inducing the translocation of NF-κB into the nucleus.[18,19] However, in contrast to the TNF-α-triggered canonical pathway, which is transient and mostly IKKβ dependent, Tax-mediated NF-κB activation is persistent and utilizes both the IKKα and IKKβ subunits.[20,21] From these observations, we speculated that oncogenic Tax-mediated activation of NF-κB is distinguishable from the canonical NF-κB activation pathway, and indeed, we have succeeded in inhibiting Tax-mediated NF-κB activation using selected sets of NEMO-mutant peptides.[11]

Those earlier studies led us to ask whether GA can inhibit Tax-mediated HMW-IKK formation and suppress NF-κB activation as has been demonstrated in the TNF-α-triggered canonical pathway. To address this, we treated ATL cell lines or HEK293 cells transfected with a Tax expression vector with GA or its less toxic derivative 17-dimethylaminoethylamino-17-demethoxygeldanamycin hydrochloride (17-DMAG).[22] We found that these HSP90 inhibitors downregulated Tax-mediated intracellular activity including the activation of NF-κB, activator protein 1 and HTLV-1 long terminal repeat (HTLV-1-LTR). These findings prompted us to investigate the molecular mechanisms by which HSP90 inhibitors disrupt Tax-mediated signaling in ATL cells. We found that the stability of Tax in ATL cells is heavily dependent on the HSP90/CDC37 chaperones and that Tax is rapidly degraded without these chaperones following the addition of HSP90 inhibitors. Apoptosis of ATL cells was also induced by GA and 17-DMAG. Finally, the oral administration of 17-DMAG to severe combined immunodeficient (SCID) mice transplanted with lymphomatous cells bearing Lck proximal promoter-driven Tax transgene (Lck-Tax) cells[23] markedly inhibited the aggressive infiltration of these Lck-Tax cells into multiple organs. The same procedure to the humanized NOG (huNOG) mice inoculated with HTLV-1-producing Jurkat cells also resulted in the suppression of *de novo* viral production and improved the survival period.

MATERIALS AND METHODS

Ethics statement

This study was carried out in strict accordance with the recommendations in the Guidelines for Proper Conduct of Animal Experiments, Science Council of Japan (http://www.scj.go.jp/en/animal/index.html). All procedures involving animals and their care were approved by the Animal Care Committee of Oita University, National Institute of Infectious Diseases and Kansai Medical University in accordance with the Regulations for Animal Experiments in Oita University (approval ID: 24-22).

Chemicals, cells and cell culture conditions

All chemicals used in this study including 17-DMAG[22] and cell lines or peripheral blood leukocytes (PBLs) were described in Supplementary Information.

Coimmunoprecipitation and immunoblot

One million cells of MT4 and C8166 treated with or without 17-DMAG and HEK293 cells transfected with each plasmid (maximum 1 μg) by FugeneHD (Roche Applied Science, Tokyo, Japan) for 40 h were lysed with coimmunoprecipitation (Co-IP) buffer. Each 200 μg of precleared (with 30 μl of protein G agarose, CalBiochem, Millipore Corporation, Billerica, MA, USA) lysates was incubated with 2 μg of rabbit polyclonal anti-HSP90 (Stressgen Bioreagents, Ann Arbor, MI, USA) or rabbit anti-FLAG antibody (Sigma-Aldrich, St Louis, MO, USA) for at least 3 h at 4° C. Antibody–protein G complexes were washed, resolved by sodium dodecyl sulfate-polyacrylamide gel electrophoresis and transferred onto a polyvinylidene difluoride membrane, and specific proteins were detected by monoclonal anti-Tax, -HSP90 (Stressgen), -Flag, -tubulin (Sigma) or polyclonal anti-IKKb (Cell Signaling Technology) antibodies, respectively.

Real-time quantitative reverse transcriptase-PCR by the LightCycler system

Total RNA from MT4 cells treated with or without 17-DMAG was isolated using ISOGEN (Wako Pure Chemical Industries, Ltd., Osaka, Japan), and contaminated DNA was removed. cDNA was constructed by the Thermoscript reverse transcriptase-PCR system (Invitrogen, Life Technologies Japan Co., Tokyo, Japan), and real-time quantitative PCRs for Tax and glucose-6-phosphate 1-dehydrogenase were performed on a Roche LC480 system (Roche) with indicated probe and primer sets.

Cell viability assay

Cell lines or PBLs from ATL patients or healthy donors were treated with 2.5 μM of 17-DMAG for 1–4 days. After every 24 h incubation, cell viabilities were counted with Cell Counting Kit (Dojindo Laboratories, Kumamoto, Japan).

Caspase-3/7 assay

Cells used in the 'cell viability assay' were also subjected for apoptosis activity with cappase-3/7 assay and GLOMAX 96 microplate luminometer (Promega KK, Tokyo, Japan).

Plasmids

The details of plasmid pSG5-Tax,[24] HSP90,[25] Cdc37,[26] CMV-Tax or LTR-Tax[11] and CoralHue-Tax or −CDC37 vectors (MBL Co. Ltd., Nagoya, Japan)[27] are described in Supplementary Information.

Luciferase assay

HEK293 cells were transfected with plasmid DNA mixture containing the reporter plasmids (NF-κB-Luc or HTLV-1-LTR-Luc[11] and RSV-β-galactosidase as a transfection indicator) and Tax expression vectors (pSG5-Tax, CMV-Tax or LTR-Tax) by FugeneHD. After 24 h incubation of the transfection, where indicated, 17-DMAG at concentrations listed in the figures was added, and cells were further incubated for 16 h. Cell lysates were subjected to the luciferase assay kit and GLOMAX 96.

Microscopic observation of cells

HEK293 cells were transfected with phmKGN-MC-Tax and phmKGC-MN-Cdc37 or its mutant −Cdc37(N200) or −Cdc37(N180) for 48 h and then treated with 1 μM of Hoechst 34442 (Sigma). Light and fluorescent (green fluorescent protein (GFP) or Hoechst 34442) microscopic observation and photography were performed by BZ-9000 Biorevo (Keyence Co. Ltd., Osaka, Japan).

Transfer of Lck-Tax transgenic cells to SCID mice and treatment with 17-DMAG

SCID mice were injected intraperitoneally with 2×10^6 Lck-Tax cells.[23] 17-DMAG was administered orally 5 days per week, with 5, 15 or 30 mg/kg for 2–3 weeks, and then mice were sacrificed for pathological examination.

HTLV-1 infection to huNOG and flow cytometric analysis of peripheral bloods

Suspension of irradiated 1×10^6 HTLV-1-producing JEX cells was inoculated intraperitoneally into huNOG mice[28] at the age between 24 and 28 weeks. Peripheral blood cells were routinely collected every 2 weeks after infection. Spleen, bone marrow and lymph node were collected, and PBLs were stained with florescent dye-conjugated antibodies against human cellular surface markers.

DNA isolation and quantification of proviral load

Genomic DNA was extracted from single cell suspension of tissue or peripheral blood followed by the conventional phenol extraction method. Proviral load was measured by quantitative PCR as previously described.[29]

Histopathological examination and immunohistochemistry

Tissues were directly fixed in the neutral buffered formalin (Sigma), embedded in paraffin, sectioned and stained with hematoxylin and eosin. Peripheral blood smears were prepared using Giemsa staining and examined by light microscopy.

For details, see Supplementary Information.